# A New Probabilistic Approach: Estimation and Monte Carlo Simulation with Applications to Time-to-Event Data

Huda M. Alshanbari [1] , **Zubair Ahmad** [2,*], **Hazem Al-Mofleh** [3] , **Clement Boateng Ampadu** [4] **and Saima K. Khosa** [5]

1 Department of Mathematical Sciences, College of Science, Princess Nourah bint Abdulrahman University, P.O. Box 84428, Riyadh 11671, Saudi Arabia
2 Department of Statistics, Quaid-i-Azam University, Islamabad 44000, Pakistan
3 Department of Mathematics, Tafila Technical University, Tafila 66110, Jordan
4 Independent Researcher, 31 Carrolton Road, Boston, MA 02132, USA
5 Department of Mathematics and Statistics, University of Saskatchewan, Saskatoon, SK S7N 5E5, Canada
* Correspondence: zahmad@stat.qau.edu.pk

Abstract: In this paper, we propose a useful method without adding any extra parameters to obtain new probability distributions. The proposed family is a combination of the two existing families of distributions and is called a weighted sine-*G* family. A two-parameter special member of the weighted sine-*G* family, using the Weibull distribution as a baseline model, is considered and investigated in detail. Some distributional properties of the weighted sine-*G* family are derived. Different estimation methods are considered to estimate the parameters of the special model of the weighted sine-*G* family. Furthermore, simulation studies based on these different methods are also provided. Finally, the applicability and usefulness of the weighted sine-*G* family are demonstrated by analyzing two data sets taken from the engineering sector.

Keywords: Weibull model; trigonometric function; family of distributions; simulation; statistical modeling; engineering data

MSC: 62N01; 62N02

1. Introduction

A challenging work for researchers is to look for flexible probability models to cater to the analysis of various types of data that possess extreme observations, such as (i) Reliability data [1], (ii) healthcare data [2], (iii) financial data [3], (iv) hydrological data [4], (v) time-to-event data [5–7], and (vi) lifetime data analysis [8,9], etc. However, the traditional distribution does not provide the best fit for the data sets, as it has extreme observations. Based on the available literature, we know that the heavy-tailed (HT) distributions have proven to be substantial for the data sets that possess extreme observations. Unfortunately, there are only a few probability models that possess HT characteristics. Therefore, researchers are always in search of new probability distributions that possess HT characteristics.

To improve the flexibility of the existing models, new methods have been suggested; see the truncated burr *XG* family [10], Fréchet Topp Leone-*G* family [11], shifted Gompertz-*G* family [12], Teissier-*G* family [13], and Gudermannian-generated family [14], among others. Thanks to these methods, they have significantly improved the fitting power of the existing distributions. However, there are certain deficiencies/problems associated with these methods, for instance, these methods involve from one to five or more additional parameters. This fact leads to estimation difficulties and re-parametrization problems. To avoid the re-parametrization problem, researchers are focusing on generating new methods without adding extra parameters. In this regard, Kumar et al. [15] suggested a useful

method using a trigonometric function, namely, a sine-*G* family. Let *X* have a sine-*G* family with a cumulative distribution function (CDF) $K(x; \boldsymbol{\vartheta})$, if it is given by

$$K(x; \boldsymbol{\vartheta}) = \sin\left(\frac{\pi}{2} G(x; \boldsymbol{\vartheta})\right), \qquad x \in \mathbb{R}, \tag{1}$$

where $\boldsymbol{\vartheta}$ is a parameter vector and $G(x; \boldsymbol{\vartheta})$ is a baseline CDF with respect to Equation (1). Since $G(x; \boldsymbol{\vartheta})$ is a baseline CDF, it must obey the following properties:

- $G(x; \boldsymbol{\vartheta})$ is a non-decreasing function.
- The maximum of $G(x; \boldsymbol{\vartheta})$ is when $x = \infty : G(\infty; \boldsymbol{\vartheta}) = 1$.
- The minimum of $G(x; \boldsymbol{\vartheta})$ is when $x = -\infty : G(-\infty; \boldsymbol{\vartheta}) = 0$.

For more contributed work using the sine function, we refer interested readers to [16–23]. Ahmad et al. [24] produced further efforts by proposing another method without any additional parameters. They used the T-*X* method to generate a weighted T-*X* (WT-*X*) family. For detailed information about the T-*X* method, we refer to [25]. The CDF $F(x; \boldsymbol{\vartheta})$ of the WT-*X* method is

$$F(x; \boldsymbol{\vartheta}) = 1 - \frac{[1 - K(x; \boldsymbol{\vartheta})]}{e^{K(x; \boldsymbol{\vartheta})}}, \qquad x \in \mathbb{R}, \tag{2}$$

where $K(x; \boldsymbol{\vartheta})$ is a baseline CDF with respect to Equation (2).

To bring further flexibility to the sine-*G* and WT-*X* methods, we propose another useful approach that possesses the HT characteristics. The proposed approach is obtained by following the spirit of the WT-*X* method along with the sine-*G* family. The proposed method may be called a weighted sine-*G* (WS-*G*) family of distributions. The key features of the WS-*G* method are (i) it has no extra parameters and (ii) it provides a useful alternative to the sine-*G* and WT-*X* methods, with possible different aims in terms of modeling.

Suppose *X* has the WS-*G* distributions with parameter vector $\boldsymbol{\vartheta}$, then, the CDF $F(x; \boldsymbol{\vartheta})$ of *X* is

$$F(x; \boldsymbol{\vartheta}) = 1 - \frac{\left[1 - \sin\left(\frac{\pi}{2} G(x; \boldsymbol{\vartheta})\right)\right]}{e^{\sin\left(\frac{\pi}{2} G(x; \boldsymbol{\vartheta})\right)}}, \qquad x \in \mathbb{R}, \tag{3}$$

with PDF

$$f(x; \boldsymbol{\vartheta}) = \left(\frac{\pi}{2}\right) \frac{g(x; \boldsymbol{\vartheta}) \cos\left(\frac{\pi}{2} G(x; \boldsymbol{\vartheta})\right)}{e^{\sin\left(\frac{\pi}{2} G(x; \boldsymbol{\vartheta})\right)}} \left[2 - \sin\left(\frac{\pi}{2} G(x; \boldsymbol{\vartheta})\right)\right], \qquad x \in \mathbb{R}, \tag{4}$$

where $\frac{d}{dx} G(x; \boldsymbol{\vartheta}) = g(x; \boldsymbol{\vartheta})$.

Furthermore, the survival function (SF) $S(x; \boldsymbol{\vartheta}) = 1 - F(x; \boldsymbol{\vartheta})$, hazard function (HF) $\frac{f(x; \boldsymbol{\vartheta})}{1 - F(x; \boldsymbol{\vartheta})}$, and cumulative HF (CHF) $H(x; \boldsymbol{\vartheta}) = -\log[1 - F(x; \boldsymbol{\vartheta})]$ are, respectively, given by

$$S(x; \boldsymbol{\vartheta}) = \frac{\left[1 - \sin\left(\frac{\pi}{2} G(x; \boldsymbol{\vartheta})\right)\right]}{e^{\sin\left(\frac{\pi}{2} G(x; \boldsymbol{\vartheta})\right)}}, \qquad x \in \mathbb{R}, \tag{5}$$

$$h(x; \boldsymbol{\vartheta}) = \left(\frac{\pi}{2}\right) \frac{g(x; \boldsymbol{\vartheta}) \cos\left(\frac{\pi}{2} G(x; \boldsymbol{\vartheta})\right)}{\left[1 - \sin\left(\frac{\pi}{2} G(x; \boldsymbol{\vartheta})\right)\right]} \left[2 - \sin\left(\frac{\pi}{2} G(x; \boldsymbol{\vartheta})\right)\right], \qquad x \in \mathbb{R}, \tag{6}$$

and

$$H(x; \boldsymbol{\vartheta}) = -\log\left(\frac{\left[1 - \sin\left(\frac{\pi}{2} G(x; \boldsymbol{\vartheta})\right)\right]}{e^{\sin\left(\frac{\pi}{2} G(x; \boldsymbol{\vartheta})\right)}}\right), \qquad x \in \mathbb{R}. \tag{7}$$

The WS-*G* method has certain advantages while implementing it in practice. The advantages of the WS-*G* method are given by

- Since the WS-*G* method has no additional parameters, it may reduce the estimation problems.
- Due to no additional parameters, the WS-*G* method avoids the re-parametrization problems.
- The WS-*G* method possesses heavy-tailed (HT) characteristics; see Section 3.

Besides the above advantages, the WS-*G* method also has certain limitations. The limitations of the WS-*G* method are

- Due to the complicated form of the PDF of the WS-*G* method, more computational efforts are required to derive its distributional properties.
- Since the quantile function of the WS-*G* method is not in an explicit form, the computer software must be implemented to generate random numbers from the WS-*G* distributions.

Based on the WS-*G* method, we study an updated form of the Weibull distribution, namely, a weighted sine-Weibull (WS-Weibull) distribution. Some basic functions of the WS-Weibull model are obtained in Section 2. Visual behaviors of the PDF of the WS-Weibull distribution are also presented. Some distributional properties of the WS-*G* method are discussed in Section 3. Section 4 is devoted to estimate the parameters of the WS-Weibull distribution using different estimation methods. The applicability of the WS-Weibull distribution is shown in Section 5. Some concluding remarks are presented in Section 6.

2. Special Model

This section offers some basic functions of a special member (i.e., WS-Weibull distribution) of the WS-*G* method with support $(0, \infty)$. Furthermore, the behaviors of the WS-Weibull distribution are also presented.

2.1. The WS-Weibull Distribution

Suppose X has the Weibull model with support $(0, \infty)$; then, its CDF $G(x; \boldsymbol{\vartheta})$ is given by

$$G(x; \boldsymbol{\vartheta}) = 1 - e^{-\lambda x^{\delta}}, \qquad x \geq 0, \delta, \lambda \in \mathbb{R}^{+}, \tag{8}$$

with PDF

$$g(x; \boldsymbol{\vartheta}) = \delta \lambda x^{\delta-1} e^{-\lambda x^{\delta}}, \qquad x > 0,$$

where $\boldsymbol{\vartheta} = (\delta, \lambda)^{\top}$. Using $G(x; \boldsymbol{\vartheta}) = 1 - e^{-\lambda x^{\delta}}$ in Equation (3), we define the CDF of the WS-Weibull model. Suppose X has the WS-Weibull model, then, its CDF $F(x; \boldsymbol{\vartheta})$ is

$$F(x; \boldsymbol{\vartheta}) = 1 - \frac{\left[1 - \sin\left(\frac{\pi}{2} \left(1 - e^{-\lambda x^{\delta}} \right) \right) \right]}{e^{\sin\left(\frac{\pi}{2} \left(1 - e^{-\lambda x^{\delta}} \right) \right)}}, \qquad x \geq 0, \tag{9}$$

with PDF

$$f(x; \boldsymbol{\vartheta}) = \frac{\delta \lambda \pi x^{\delta-1} e^{-\lambda x^{\delta}} \cos\left(\frac{\pi}{2} \left(1 - e^{-\lambda x^{\delta}} \right) \right)}{2 e^{\sin\left(\frac{\pi}{2} \left(1 - e^{-\lambda x^{\delta}} \right) \right)}} \left[2 - \sin\left(\frac{\pi}{2} \left(1 - e^{-\lambda x^{\delta}} \right) \right) \right]. \tag{10}$$

For different values of δ and λ, Figure 1 offers different plots: $f(x; \boldsymbol{\vartheta})$ (WS-Weibull), $g(x; \boldsymbol{\vartheta})$ (Weibull), and $k(x; \boldsymbol{\vartheta})$ (sin-Weibull) distributions. Figure 1 shows that the shapes of $f(x; \boldsymbol{\vartheta})$, $g(x; \boldsymbol{\vartheta})$ and $k(x; \boldsymbol{\vartheta})$ have different forms such as right-skewed, symmetrical, left-skewed, and decreasing.
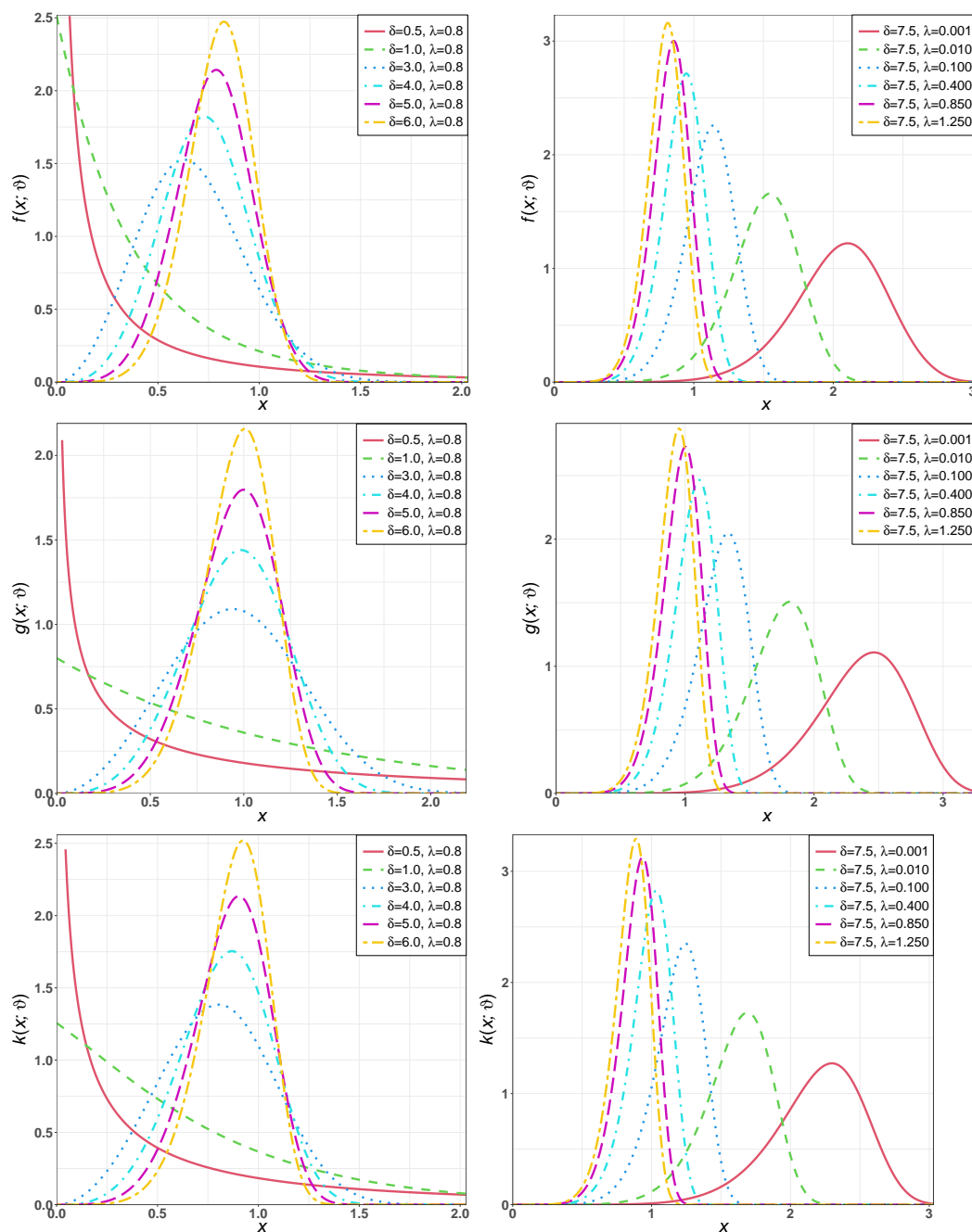
Figure 1. Plots of $f(x; \boldsymbol{\vartheta})$ of the WS-Weibull distribution for different values of δ and λ.

Table 1 shows the summation formula exact values for the PDFs of the WS-Weibull, Weibull, and sin-Weibull distributions for different values of x, δ, and λ at truncated N terms. From Table 1 and Figure 1, it can be concluded that the PDF value of the WS-Weibull distribution is less than the PDF values of the Weibull and sin-Weibull distributions for the same x, δ and λ. These results are calculated by using R software (version 4.2.2).

Furthermore, the SF, CHF, and HF of the WS-Weibull distribution are

$$S(x; \boldsymbol{\vartheta}) = \frac{\left[1 - \sin\left(\frac{\pi}{2}\left(1 - e^{-\lambda x^{\delta}}\right)\right)\right]}{e^{\sin\left(\frac{\pi}{2}\left(1 - e^{-\lambda x^{\delta}}\right)\right)}}, \tag{11}$$

$$H(x;\boldsymbol{\vartheta}) = -\log\left(\frac{\left[1 - \sin\left(\frac{\pi}{2}\left(1 - e^{-\lambda x^\delta}\right)\right)\right]}{e^{\sin\left(\frac{\pi}{2}\left(1 - e^{-\lambda x^\delta}\right)\right)}}\right),\tag{12}$$

and

$$h(x;\boldsymbol{\vartheta}) = \frac{\delta\lambda\pi x^{\delta-1}e^{-\lambda x^\delta}\cos\left(\frac{\pi}{2}\left(1 - e^{-\lambda x^\delta}\right)\right)}{2\left[1 - \sin\left(\frac{\pi}{2}\left(1 - e^{-\lambda x^\delta}\right)\right)\right]}\left[2 - \sin\left(\frac{\pi}{2}\left(1 - e^{-\lambda x^\delta}\right)\right)\right],\tag{13}$$

respectively.

Table 1. The summation formula and the exact value for the PDFs of WS-Weibull, Weibull, and sin-Weibull distributions for different values of x, δ, and λ at truncated N terms.

x	δ	λ	N	WS-Weibull		sin-Weibull		Weibull
				Summation	**Exact Value**	**Summation**	**Exact Value**	**Exact Value**
0.5	0.8	1.2	2	0.4090627		0.6170058		
			4	0.3950064	0.3946863	0.6167320	0.6167320	0.5535454
			10	0.3946863		0.6167320		
		2.2	2	0.1841287		0.3880394		
			4	0.1718327	0.1714237	0.3855453	0.3855445	0.5714233
			10	0.1714237		0.3855445		
	1.5	1.2	2	1.0064660		1.1198750		
			4	0.9908311	0.9906327	1.1198280	1.1198280	0.8327257
			10	0.9906327		1.1198280		
		2.2	2	0.6842317		1.1132750		
			4	0.6566751	0.6559729	1.1124090	1.1124090	1.0720057
			10	0.6559729		1.1124090		
1.0	0.8	1.2	2	0.1009522		0.2080368		
			4	0.0945207	0.0943092	0.2069571	0.2069568	0.2891464
			10	0.0943092		0.2069568		
		2.2	2	0.0230105		0.0560985		
			4	0.0201815	0.0201114	0.0530495	0.0530471	0.1950136
			10	0.0201114		0.0530471		
	1.5	1.2	2	0.1892854		0.3900691		
			4	0.1772264	0.1768297	0.3880446	0.3880440	0.5421496
			10	0.1768297		0.3880440		
		2.2	2	0.0431448		0.1051847		
			4	0.0378403	0.0377088	0.0994678	0.0994634	0.3656504
			10	0.0377088		0.0994634		
2.5	0.8	1.2	2	0.0058948		0.0145537		
			4	0.0049978	0.0049798	0.0133140	0.0133129	0.0657602
			10	0.0049798		0.0133129		
		2.2	2	0.0003286		0.0008248		
			4	0.0001409	0.0001402	0.0003815	0.0003809	0.0150408
			10	0.0001402		0.0003809		
	1.5	1.2	2	0.0005063		0.0012709		
			4	0.0001970	0.0001960	0.0005335	0.0005326	0.0247858
			10	0.0001960		0.0005326		
		2.2	2	0.0000110		0.0000277		
			4	0.0000001	0.0000001	0.0000004	0.0000004	0.0008725
			10	0.0000001		0.0000004		

Figure 2 displays HF plots for the WS-Weibull distribution for various δ and λ values; it can be observed that the HF shapes of the WS-Weibull distribution can be increasing, decreasing, and unimodal.
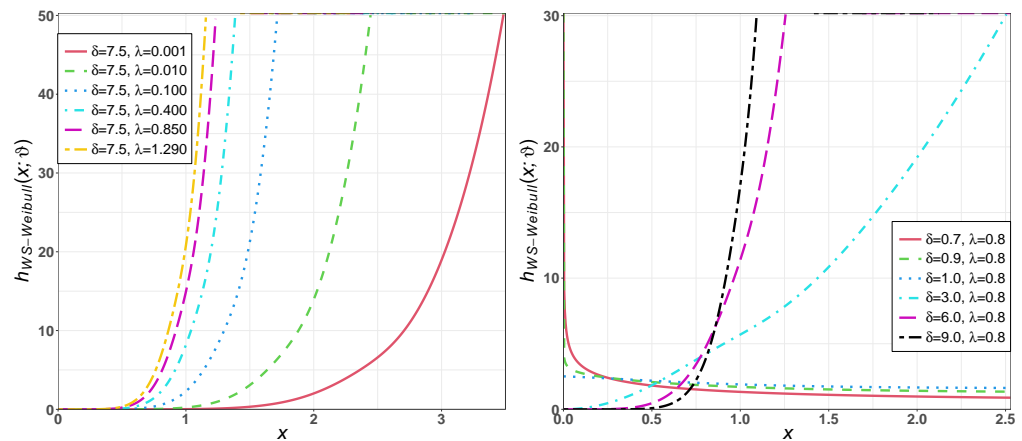
Figure 2. Plots of $h_{WS-Weibull}(x; \boldsymbol{\vartheta})$ of the WS-Weibull distribution for different values of δ and λ.

2.2. The Behaviors of the PDF and HF of the WS-Weibull Model

Here, we discuss the behaviors of the PDF and HF of the WS-Weibull distribution. The behaviors of the PDF of the WS-Weibull distribution when $x \to 0$ and $x \to \infty$ are, respectively, given by

$$\lim_{x \to 0} f(x; \boldsymbol{\vartheta}) = \begin{cases} \infty & \text{if } \delta < 1, \\ \pi\lambda & \text{if } \delta = 1, \\ 0 & \text{if } \delta > 1, \end{cases}$$

and

$$\lim_{x \to \infty} f(x; \boldsymbol{\vartheta}) = 0.$$

Similarly, the behavior of the HF defined in Equation (13) when $x \to 0$ and $x \to \infty$ are, respectively, given by

$$\lim_{x \to 0} h_{WS-Weibull}(x; \boldsymbol{\vartheta}) = \begin{cases} \infty & \text{if } \delta < 1, \\ \pi\lambda & \text{if } \delta = 1, \\ 0 & \text{if } \delta > 1, \end{cases}$$

and

$$\lim_{x \to \infty} h_{WS-Weibull}(x; \boldsymbol{\vartheta}) = \begin{cases} 0 & \text{if } \delta < 1, \\ 2\lambda & \text{if } \delta = 1, \\ \infty & \text{if } \delta > 1. \end{cases}$$

Now, we compare the behaviors of the HF of the Weibull, sin-Weibull (as a special case from the family in Equation (1)), and WS-Weibull distributions. The behavior of the HF of the Weibull distribution when $x \to 0$ and $x \to \infty$ are, respectively, given by

$$\lim_{x \to 0} h_{Weibull}(x; \delta, \lambda) = \begin{cases} \infty & \text{if } \delta < 1, \\ \lambda & \text{if } \delta = 1, \\ 0 & \text{if } \delta > 1, \end{cases}$$

and

$$\lim_{x \to \infty} h_{Weibull}(x; \delta, \lambda) = \begin{cases} 0 & \text{if } \delta < 1, \\ \lambda & \text{if } \delta = 1, \\ \infty & \text{if } \delta > 1. \end{cases}$$

Now, the behavior of the HF of the sin-Weibull distribution when $x \to 0$ and $x \to \infty$ are, respectively, given by

$$\lim_{x \to 0} h_{\sin-Weibull}(x; \delta, \lambda) = \begin{cases} \infty & \text{if } \delta < 1, \\ \frac{\pi\lambda}{2} & \text{if } \delta = 1, \\ 0 & \text{if } \delta > 1, \end{cases}$$

and

$$\lim_{x \to \infty} h_{\sin-Weibull}(x; \delta, \lambda) = \begin{cases} 0 & \text{if } \delta < 1, \\ 2\lambda & \text{if } \delta = 1, \\ \infty & \text{if } \delta > 1. \end{cases}$$

From the above results, we can conclude that the HF behaviors of these distributions are roughly similar.

Table 2 displays the summary of the HF limits for the WS-Weibull, Weibull, and sin-Weibull distributions. From the above mathematical results and numerical illustration in Table 2, we can conclude that the HF behaviors of these distributions are roughly similar.

Table 2. The summary of the HF limits for the WS-Weibull, Weibull, and sin-Weibull distributions.

Distributions	Limit as $x \to 0$			Limit as $x \to \infty$		
	$\delta < 1$	$\delta = 1$	$\delta > 1$	$\delta < 1$	$\delta = 1$	$\delta > 1$
WS-Weibull	∞	$\pi\lambda$	0	0	2λ	∞
Weibull	∞	λ	0	0	λ	∞
sin-Weibull	∞	$\frac{\pi}{2}\lambda$	0	0	2λ	∞

3. Distributional Properties

Here, we give some distributional properties associated with the proposed method.

3.1. Expansion for the CDF

Using the power series representation for $\sin(x)$ and e^x, we can write the CDF as

$$F(x; \boldsymbol{\vartheta}) = 1 - \frac{1 - \sum_{n=0}^{\infty} (-1)^n \dfrac{\left(\frac{\pi}{2} G(x; \boldsymbol{\vartheta})\right)^{2n+1}}{(2n+1)!}}{\sum_{n=0}^{\infty} \dfrac{\left(\sin\left(\frac{\pi}{2} G(x; \boldsymbol{\vartheta})\right)\right)^n}{n!}}.$$

3.2. Expansion for the PDF

Using the power series representation for $\sin(x)$, $\cos(x)$, and e^x we can write the PDF as

$$f(x; \boldsymbol{\vartheta}) = \frac{\pi}{2} g(x; \boldsymbol{\vartheta}) \frac{\sum_{n=0}^{\infty} \dfrac{(-1)^n \left(\frac{\pi}{2} G(x; \vartheta)\right)^{2n}}{2n!}}{\sum_{n=0}^{\infty} \dfrac{\left(\sin\left(\frac{\pi}{2} G(x; \vartheta)\right)\right)^n}{n!}} \left(2 - \sum_{n=0}^{\infty} (-1)^n \dfrac{\left(\frac{\pi}{2} G(x; \vartheta)\right)^{2n+1}}{(2n+1)!}\right).$$

3.3. Quantile Function

We solve for $Q(p)$ in the following, where $0 < p < 1$,

$$p = 1 - \frac{1 - \sin\left(\frac{\pi}{2}G(Q(p))\right)}{e^{\sin\left(\frac{\pi}{2}G(Q(p))\right)}}.$$

After some algebraic manipulations, we arrive at

$$Q(p) = G^{-1}\left[-\frac{2}{\pi}\sin^{-1}(1 - W_{-1}((1-p)e))\right],$$

where $W_{-1}(\cdot)$ is the negative branch of the Lambert function.

3.4. Moment-Generating Function

The moment-generating function is defined as

$$M_X(t) = \sum_{r=0}^{\infty} \frac{t^r}{r!} \int_0^{\infty} x^r f(x)dx.$$

For the given family of distributions, we have

$$M_X(t) = \frac{\pi}{2} \sum_{r=0}^{\infty} \frac{t^r}{r!} \int_0^{\infty} x^r g(x;\vartheta) \frac{\sum_{n=0}^{\infty} \frac{(-1)^n \left(\frac{\pi}{2}G(x;\vartheta)\right)^{2n}}{2n!}}{\sum_{n=0}^{\infty} \frac{\left(\sin\left(\frac{\pi}{2}G(x;\vartheta)\right)\right)^n}{n!}}$$
$$\times \left(2 - \sum_{n=0}^{\infty} (-1)^n \frac{\left(\frac{\pi}{2}G(x;\vartheta)\right)^{2n+1}}{(2n+1)!}\right) dx.$$

3.5. Incomplete Moments

The incomplete moments are defined by

$$M_r(x) = \int_0^x x^r f(x)dx.$$

For the given distribution, we have

$$M_r(x) = \frac{\pi}{2} \int_0^x x^r g(x;\vartheta) \frac{\sum_{n=0}^{\infty} \frac{(-1)^n \left(\frac{\pi}{2}G(x;\vartheta)\right)^{2n}}{2n!}}{\sum_{n=0}^{\infty} \frac{\left(\sin\left(\frac{\pi}{2}G(x;\vartheta)\right)\right)^n}{n!}}$$
$$\times \left(2 - \sum_{n=0}^{\infty} (-1)^n \frac{\left(\frac{\pi}{2}G(x;\vartheta)\right)^{2n+1}}{(2n+1)!}\right) dx.$$

3.6. The rth Non-Central Moment

The rth non-central moment is defined as

$$\mu_r' = \int_0^{\infty} x^r f(x)dx.$$

For the proposed family, we have

$$\mu'_r = \frac{\pi}{2} \int_0^\infty x^r g(x;\vartheta) \frac{\sum_{n=0}^\infty \frac{(-1)^n \left(\frac{\pi}{2} G(x;\vartheta)\right)^{2n}}{2n!}}{\sum_{n=0}^\infty \frac{\left(\sin\left(\frac{\pi}{2} G(x;\vartheta)\right)\right)^n}{n!}} \left(2 - \sum_{n=0}^\infty (-1)^n \frac{\left(\frac{\pi}{2} G(x;\vartheta)\right)^{2n+1}}{(2n+1)!}\right) dx.$$

Now, we compute the above integral numerically. Table 3 displays the summation formula and the numerical integration (NI) values for the rth non-central moments of the WS-Weibull, Weibull, and sin-Weibull distributions for different values of r, δ, and λ at truncated N terms. From the given results in Table 3, it can be concluded that the rth non-central moments of the WS-Weibull distribution is less than the rth non-central moments of the Weibull and sin-Weibull distributions for the same r, δ, and λ.

Table 3. The summation formula and the numerical integration values for the rth non-central moments of the WS-Weibull, Weibull, and sin-Weibull distributions for different values of r, δ, and λ at truncated N terms.

r	δ	λ	N	WS-Weibull		sin-Weibull		Weibull
				Summation	NI	Summation	NI	Exact Integration
1.0	0.8	1.2	2	0.2712448		0.4416135		
			4	0.2560016	0.2556559	0.4294283	0.4294168	0.9020998
			10	0.2556559		0.4294168		
		2.2	2	0.1271481		0.2070096		
			4	0.1200027	0.1198406	0.2012978	0.2012924	0.4228660
			10	0.1198406		0.2012924		
	1.5	1.2	2	0.4124430		0.5530663		
			4	0.3983605	0.3980281	0.5457003	0.5456939	0.7994250
			10	0.3980281		0.5456939		
		2.2	2	0.2753402		0.3692180		
			4	0.2659389	0.2657171	0.3643006	0.3642963	0.5336831
			10	0.2657171		0.3642963		
2.0	0.8	1.2	2	0.2331464		0.4881900		
			4	0.2027422	0.2022463	0.4433054	0.4432577	2.1067990
			10	0.2022463		0.4432577		
		2.2	2	0.0512301		0.1072717		
			4	0.0445493	0.0444403	0.0974091	0.0973986	0.4629345
			10	0.0444403		0.0973986		
	1.5	1.2	2	0.2609388		0.4347446		
			4	0.2453182	0.2449682	0.4215772	0.4215647	0.9336954
			10	0.2449682		0.4215647		
		2.2	2	0.1162921		0.1937518		
			4	0.1093305	0.1091745	0.1878835	0.1878779	0.4161181
			10	0.1091745		0.1878779		
3.0	0.8	1.2	2	0.4160335		0.9762510		
			4	0.3061227	0.3051022	0.7563797	0.7561286	8.3717721
			10	0.3051022		0.7561286		
		2.2	2	0.0428522		0.1005556		
			4	0.0315312	0.0314261	0.0779084	0.0778826	0.8623072
			10	0.0314261		0.0778826		
	1.5	1.2	2	0.2236855		0.4328695		
			4	0.2024038	0.2019931	0.4071599	0.4071336	1.3888889
			10	0.2019931		0.4071336		
		2.2	2	0.0665511		0.1287876		
			4	0.0602193	0.0600971	0.1211385	0.1211307	0.4132231
			10	0.0600971		0.1211307		

3.7. Rényi Entropy

The Rényi entropy of a random variable X is a measure of the variation of uncertainty. It is defined by

$$I_v(X) = (1-v)^{-1} \log\left(\int_{-\infty}^{\infty} f(x)^v dx\right), \quad v > 0 \text{ and } v \neq 1.$$

Using the WS-Weibull density, we obtain

$$f(x;\boldsymbol{\vartheta})^v = \left(\frac{\delta\lambda\pi}{2}\right)^v \frac{x^{v(\delta-1)}e^{-\lambda vx^\delta}\left(\cos\left(\frac{\pi}{2}\left(1-e^{-\lambda x^\delta}\right)\right)\right)^v}{e^{v\sin\left(\frac{\pi}{2}\left(1-e^{-\lambda x^\delta}\right)\right)}}\left[2-\sin\left(\frac{\pi}{2}\left(1-e^{-\lambda x^\delta}\right)\right)\right]^v.$$

Then, the Rényi entropy of the WS-Weibull density takes the form

$$I_v(X) = (1-v)^{-1}\log\Bigg\{\left(\frac{\delta\lambda\pi}{2}\right)^v\int_0^\infty \frac{x^{v(\delta-1)}e^{-\lambda vx^\delta}\left(\cos\left(\frac{\pi}{2}\left(1-e^{-\lambda x^\delta}\right)\right)\right)^v}{e^{v\sin\left(\frac{\pi}{2}\left(1-e^{-\lambda x^\delta}\right)\right)}}$$

$$\times\left[2-\sin\left(\frac{\pi}{2}\left(1-e^{-\lambda x^\delta}\right)\right)\right]^v dx\Bigg\}.$$

Table 4 displays the summation formula and the NI values for the Rényi entropy of the WS-Weibull, Weibull, and sin-Weibull distributions for different values of v, δ, and λ at truncated N terms. From Table 4, we can observe that the values of the Rényi entropy for the WS-Weibull distribution is less than the Rényi values of the Weibull and sin-Weibull distributions for the same v, δ, and λ.

Table 4. The summation formula and the numerical integration values for the Rényi entropy of WS-Weibull, Weibull, and sin-Weibull distributions for different values of v, δ, and λ at truncated N terms.

v	δ	λ	N	WS-Weibull		sin-Weibull		Weibull
				Summation	**NI**	**Summation**	**NI**	**Exact Value**
0.5	0.8	1.2	2	0.3572427		0.7321667		
			4	0.2645767	0.2631333	0.6566993	0.6564579	1.4347754
			10	0.2631333		0.6564579		
		2.2	2	−0.4004269		−0.0255028		
			4	−0.4930927	−0.4945364	−0.1009705	−0.1012118	0.6771066
			10	−0.4945364		−0.1012118		
	1.5	1.2	2	0.3055993		0.4904644		
			4	0.2511143	0.2501745	0.4488667	0.4487522	0.8705198
			10	0.2501745		0.4487522		
		2.2	2	−0.0984913		0.0863738		
			4	−0.1529758	−0.1539160	0.0447768	0.0446617	0.4664292
			10	−0.1539160		0.0446617		
2.0	0.8	1.2	2	−1.0818547		−0.3444082		
			4	−1.0767934	−1.0767260	−0.3439980	−0.3439978	0.3118210
			10	−1.0767261		−0.3439978		
		2.2	2	−1.8395245		−1.1020779		
			4	−1.8344632	−1.8343958	−1.1016677	−1.1016675	−0.4458487
			10	−1.8343958		−1.1016675		
	1.5	1.2	2	−0.2044980		0.1123635		
			4	−0.1918153	−0.1916098	0.1136098	0.1136103	0.5103751
			10	−0.1916098		0.1136103		
		2.2	2	−0.6085886		−0.2917271		
			4	−0.5959058	−0.5957003	−0.2904808	−0.2904803	0.1062845
			10	−0.5957004		−0.2904803		

Table 4. *Cont.*

v	δ	λ	N	WS-Weibull		sin-Weibull		Weibull
				Summation	**NI**	**Summation**	**NI**	**Exact Value**
4.0	0.8	1.2	2	−1.7438683		−0.9049445		
			4	−1.7437275	−1.7437268	−0.9049410	−0.9049410	−0.3185747
			10	−1.7437268		−0.9049410		
		2.2	2	-2.5015382		−1.6626142		
			4	-2.5013973	-2.5013966	−1.6626107	−1.6626107	−1.0762445
			10	-2.5013966		−1.6626107		
	1.5	1.2	2	−0.3274484		0.0083556		
			4	−0.3237034	−0.3236696	0.0085064	0.0085064	0.3971834
			10	−0.3236696		0.0085064		
		2.2	2	−0.7315390		−0.3957349		
			4	−0.7277940	−0.7277602	−0.3955842	−0.3955842	−0.0069071
			10	−0.7277602		−0.3955842		

3.8. The HT Characteristics of the WS-G Method

Here, we provide a complete mathematical description to derive the HT characteristics of the WS-*G* method.

3.8.1. The Regularly Varying Characteristics of the WS-*G* Method

The regularly varying characteristics (RVC) play an important role in defining HT distributions. This subsection offers the RVC of the WS-*G* method. Using Karamata's theorem [26], in terms of SF $S(x; \boldsymbol{\vartheta})$, we have

Theorem 1. *Suppose* $\bar{K}(x; \boldsymbol{\vartheta}) = 1 - K(x; \boldsymbol{\vartheta})$ *represents the SF of a regularly varying function (RVF), then* $S(x; \boldsymbol{\vartheta}) = 1 - F(x; \boldsymbol{\vartheta})$ *also represents the SF of a RVF.*

Proof. Assume $\lim_{x \to \infty} \frac{\bar{K}(tx; \boldsymbol{\vartheta})}{\bar{K}(x; \boldsymbol{\vartheta})} = \tau(t)$ is a finite and nonzero function $\forall \ t > 0$. Then, by incorporating the expression in Equation (5), we have

$$\frac{S(tx; \boldsymbol{\vartheta})}{S(x; \boldsymbol{\vartheta})} = \frac{\left[1 - \sin\left(\frac{\pi}{2}G(tx; \boldsymbol{\vartheta})\right)\right]}{e^{\sin\left(\frac{\pi}{2}G(tx; \boldsymbol{\vartheta})\right)}} \times \frac{e^{\sin\left(\frac{\pi}{2}G(x; \boldsymbol{\vartheta})\right)}}{\left[1 - \sin\left(\frac{\pi}{2}G(x; \boldsymbol{\vartheta})\right)\right]},$$

$$\frac{S(tx; \boldsymbol{\vartheta})}{S(x; \boldsymbol{\vartheta})} = \frac{\left[1 - \sin\left(\frac{\pi}{2}G(tx; \boldsymbol{\vartheta})\right)\right]}{\left[1 - \sin\left(\frac{\pi}{2}G(x; \boldsymbol{\vartheta})\right)\right]} \times \frac{e^{\sin\left(\frac{\pi}{2}G(x; \boldsymbol{\vartheta})\right)}}{e^{\sin\left(\frac{\pi}{2}G(tx; \boldsymbol{\vartheta})\right)}},$$

$$\frac{S(tx; \boldsymbol{\vartheta})}{S(x; \boldsymbol{\vartheta})} = \frac{[1 - K(tx; \boldsymbol{\vartheta})]}{[1 - K(x; \boldsymbol{\vartheta})]} \times \frac{e^{\sin\left(\frac{\pi}{2}G(x; \boldsymbol{\vartheta})\right)}}{e^{\sin\left(\frac{\pi}{2}G(tx; \boldsymbol{\vartheta})\right)}}. \tag{14}$$

Applying $\lim_{x \to \infty}$ on both sides of Equation (14), we obtain

$$\lim_{x \to \infty} \frac{S(tx; \boldsymbol{\vartheta})}{S(x; \boldsymbol{\vartheta})} = \lim_{x \to \infty} \frac{[1 - K(tx; \boldsymbol{\vartheta})]}{[1 - K(x; \boldsymbol{\vartheta})]} \times \frac{e^{\sin\left(\frac{\pi}{2}G(x; \boldsymbol{\vartheta})\right)}}{e^{\sin\left(\frac{\pi}{2}G(tx; \boldsymbol{\vartheta})\right)}},$$

$$\lim_{x \to \infty} \frac{S(tx; \boldsymbol{\vartheta})}{S(x; \boldsymbol{\vartheta})} = \tau(t) \times \frac{e^{\sin\left(\frac{\pi}{2}G(\infty; \boldsymbol{\vartheta})\right)}}{e^{\sin\left(\frac{\pi}{2}G(t\infty; \boldsymbol{\vartheta})\right)}}. \tag{15}$$

As we mentioned earlier, $G(\infty; \boldsymbol{\vartheta}) = 1$. Thus, from Equation (15), we obtain

$$\lim_{x \to \infty} \frac{S(tx; \boldsymbol{\vartheta})}{S(x; \boldsymbol{\vartheta})} = \tau(t) \times \frac{e^{\sin\left(\frac{\pi}{2}\right)}}{e^{\sin\left(\frac{\pi}{2}\right)}},$$

$$\lim_{x \to \infty} \frac{S(tx; \boldsymbol{\vartheta})}{S(x; \boldsymbol{\vartheta})} = \tau(t). \tag{16}$$

The expression in Equation (16) is finite and nonzero $\forall \, t > 0$. Therefore, $S(x; \boldsymbol{\vartheta})$ is an RVF. $\square$

3.8.2. The Regular Variational Result

Suppose X possesses the power law behavior, then, we have

$$\bar{K}(x; \boldsymbol{\vartheta}) = 1 - K(x; \boldsymbol{\vartheta}) = \mathbb{P}(X > x) \sim x^{-\sigma}.$$

By implementing the results of Karamata's characterization theorem, we can write $S(x; \boldsymbol{\vartheta})$ as

$$S(x; \boldsymbol{\vartheta}) = x^{-\sigma} L(x),$$

where $L(x)$ is a slowly varying function (SVF). Note that

$$S(x; \boldsymbol{\vartheta}) = \frac{[1 - K(x; \boldsymbol{\vartheta})]}{e^{\sin\left(\frac{\pi}{2} G(tx; \boldsymbol{\vartheta})\right)}} \tag{17}$$

Since $1 - K(x; \boldsymbol{\vartheta}) \sim x^{-\sigma}$, from Equation (17), we obtain

$$S(x; \boldsymbol{\vartheta}) = \frac{x^{-\sigma}}{e^{1 - x^{-\sigma}}},$$

$$S(x; \boldsymbol{\vartheta}) = x^{-\sigma} L(x),$$

where $L(x) = \frac{1}{e^{1 - x^{-\sigma}}}$.

Now, if we demonstrated that $L(x)$ is a SVF, the RVC of the WS-*G* method derived above is true. In order to demonstrate that $L(x)$ is a SVF, we must show that

$$\lim_{x \to \infty} \frac{L(tx)}{L(x)} = 1, \quad \forall \, t > 0. \tag{18}$$

Now, we use

$$\frac{L(tx)}{L(x)} = \frac{\frac{1}{e^{1 - (tx)^{-\sigma}}}}{\frac{1}{e^{1 - x^{-\sigma}}}},$$

$$\frac{L(tx)}{L(x)} = \frac{e^{1 - x^{-\sigma}}}{e^{1 - (tx)^{-\sigma}}}. \tag{19}$$

Appling $\lim_{x \to \infty}$ on both sides of Equation (19), we obtain

$$\lim_{x \to \infty} \frac{L(tx)}{L(x)} = \lim_{x \to \infty} \frac{e^{1 - x^{-\sigma}}}{e^{1 - (tx)^{-\sigma}}},$$

$$\lim_{x \to \infty} \frac{L(tx)}{L(x)} = 1.$$

4. Eight Estimation Methods for the WS-Weibull Parameters

Eight estimation methods have been opted for in this section to estimate the WS-Weibull parameters, namely, the weighted least-squares (WLSE), ordinary least-squares (OLSE), maximum likelihood (MLE), the maximum product of spacing (MPSE), Cramér-von Mises (CVME), Anderson-Darling (ADE), right-tail Anderson-Darling (RADE), and percentile estimator (PCE).

4.1. Maximum Likelihood

Suppose that $x_1, x_2, ..., x_n$ are given values of a random sample of size n from the WS-Weibull distribution with parameters δ and λ. The log-likelihood function for the WS-Weibull model with PDF in (10) is given by

$$
\begin{aligned}
\ell(\boldsymbol{\vartheta}) = {} & n \log\left(\frac{\pi}{2}\right) + n \log(\delta\lambda) - \lambda \sum_{i=1}^{n} x_i^{\delta} + \sum_{i=1}^{n} \log\left(2 - \sin\left(\frac{\pi}{2}\left(1 - e^{-\lambda x_i^{\delta}}\right)\right)\right) \\
& + (\delta - 1) \sum_{i=1}^{n} \log(x_i) - \sum_{i=1}^{n} \sin\left(\frac{\pi}{2}\left(1 - e^{-\lambda x_i^{\delta}}\right)\right) \\
& + \sum_{i=1}^{n} \log\left(\cos\left(\frac{\pi}{2}\left(1 - e^{-\lambda x_i^{\delta}}\right)\right)\right),
\end{aligned}
\tag{20}
$$

where $\boldsymbol{\vartheta} = (\delta, \lambda)^{\top}$. The function provided in Equation (20) can be numerically solved by using the Newton–Raphson method (iteration method). The partial derivatives of Equation (9) with respect to the parameters δ and λ are

$$
\begin{aligned}
\frac{\partial \ell}{\partial \delta} = {} & \frac{n}{\delta} - \lambda \sum_{i=1}^{n} x_i^{\delta} \log(x_i) - \frac{\pi}{2} \lambda \sum_{i=1}^{n} x_i^{\delta} \log(x_i) e^{-\lambda x_i^{\delta}} \tan\left(\frac{\pi}{2}\left(1 - e^{-\lambda x_i^{\delta}}\right)\right) \\
& - \frac{\pi}{2} \lambda \sum_{i=1}^{n} x_i^{\delta} \log(x_i) e^{-\lambda x_i^{\delta}} \cos\left(\frac{\pi}{2}\left(1 - e^{-\lambda x_i^{\delta}}\right)\right) + \sum_{i=1}^{n} \log(x_i) \\
& - \frac{\pi}{2} \lambda \sum_{i=1}^{n} \frac{x_i^{\delta} \log(x_i) e^{-\lambda x_i^{\delta}} \cos\left(\frac{\pi}{2}\left(1 - e^{-\lambda x_i^{\delta}}\right)\right)}{2 - \sin\left(\frac{\pi}{2}\left(1 - e^{-\lambda x_i^{\delta}}\right)\right)},
\end{aligned}
$$

and

$$
\begin{aligned}
\frac{\partial \ell}{\partial \lambda} = {} & \frac{n}{\lambda} - \frac{\pi}{2} \sum_{i=1}^{n} x_i^{\delta} e^{-\lambda x_i^{\delta}} \cos\left(\frac{\pi}{2}\left(1 - e^{-\lambda x_i^{\delta}}\right)\right) - \frac{\pi}{2} \sum_{i=1}^{n} x_i^{\delta} e^{-\lambda x_i^{\delta}} \tan\left(\frac{\pi}{2}\left(1 - e^{-\lambda x_i^{\delta}}\right)\right) \\
& - \frac{\pi}{2} \sum_{i=1}^{n} \frac{x_i^{\delta} e^{-\lambda x_i^{\delta}} \cos\left(\frac{\pi}{2}\left(1 - e^{-\lambda x_i^{\delta}}\right)\right)}{2 - \sin\left(\frac{\pi}{2}\left(1 - e^{-\lambda x_i^{\delta}}\right)\right)} - \sum_{i=1}^{n} x_i^{\delta}.
\end{aligned}
$$

By setting $\frac{\partial \ell}{\partial \delta} = 0$ and $\frac{\partial \ell}{\partial \lambda} = 0$, one can solve them numerically to obtain the MLEs of the parameters δ and λ.

4.2. Ordinary and Weighted Least-Squares

The OLSE of the WS-Weibull parameters can be obtained by minimizing the following function with respect to δ and λ,

$$
V(\delta, \lambda) = \sum_{i=1}^{n} \left[F(x_i | \delta, \lambda) - \frac{i}{n+1} \right]^2.
$$

Further, the OLSE of the WS-Weibull parameters can also be obtained by solving the non-linear equation

$$
\sum_{i=1}^{n} \left[F(x_i | \delta, \lambda) - \frac{i}{n+1} \right] \Delta_s(x_i | \delta, \lambda) = 0, \quad s = 1, 2,
$$

where

$$
\begin{aligned}
\Delta_1(x_{(i)}|\delta,\lambda) =& \frac{\partial}{\partial\delta}F(x_{(i)}|\delta,\lambda)\\
=& \lambda\frac{\pi}{2}x_{(i)}^{\delta}\log(x_{(i)})\cos\left(\frac{\pi}{2}\left(1-e^{-\lambda x_{(i)}^{\delta}}\right)\right)e^{-\lambda x_{(i)}^{\delta}-\sin\left(\frac{\pi}{2}\left(1-e^{-\lambda x_{(i)}^{\delta}}\right)\right)}\\
&\times\left[2-\sin\left(\frac{\pi}{2}\left(1-e^{-\lambda x_{(i)}^{\delta}}\right)\right)\right],
\end{aligned}
\tag{21}
$$

and

$$
\begin{aligned}
\Delta_2(x_{(i)}|\delta,\lambda) =& \frac{\partial}{\partial\lambda}F(x_{(i)}|\delta,\lambda)\\
=& \frac{\pi}{2}x_{(i)}^{\delta}\cos\left(\frac{\pi}{2}\left(1-e^{-\lambda x_{(i)}^{\delta}}\right)\right)e^{-\lambda x_{(i)}^{\delta}-\sin\left(\frac{\pi}{2}\left(1-e^{-\lambda x_{(i)}^{\delta}}\right)\right)}\\
&\times\left[2-\sin\left(\frac{\pi}{2}\left(1-e^{-\lambda x_{(i)}^{\delta}}\right)\right)\right].
\end{aligned}
\tag{22}
$$

The WLSE of the WS-Weibull parameters are obtained by minimizing the following

$$
W(\delta,\lambda) = \sum_{i=1}^{n}\frac{(n+1)^2(n+2)}{i(n-i+1)}\left[F(x_i|\delta,\lambda)-\frac{i}{n+1}\right]^2,
$$

with respect to δ and λ. Moreover, the WLSE can also be obtained by solving the non-linear equation

$$
\sum_{i=1}^{n}\frac{(n+1)^2(n+2)}{i(n-i+1)}\left[F(x_i|\delta,\lambda)-\frac{i}{n+1}\right]\Delta_s(x_i)=0, \quad s=1,2,
$$

where $\Delta_1(\cdot|\delta,\lambda)$ and $\Delta_2(\cdot|\delta,\lambda)$ are, respectively, defined in Equations (21) and (22).

4.3. Maximum Product of Spacing

The MPSE is considered an alternative to the maximum likelihood method. Let $D_i(\delta,\lambda)=F\left(x_{(i)}|\delta,\lambda\right)-F\left(x_{(i-1)}|\delta,\lambda\right)$, for $i=1,2,\ldots,n+1$, be the uniform spacing of a random sample from the WS-Weibull model, where $F\left(x_{(0)}|\delta,\lambda\right)=0$, $F\left(x_{(n+1)}|\delta,\lambda\right)=1$ and $\sum_{i=1}^{n+1}D_i(\delta,\lambda)=1$. The MPSE of the WS-Weibull parameters can be obtained by maximizing the "geometric mean of the spacing"

$$
G(\delta,\lambda) = \left[\prod_{i=1}^{n+1}D_i(\delta,\lambda)\right]^{\frac{1}{n+1}},
$$

with respect to δ and λ, or by maximizing the "logarithm of the geometric mean" of sample-spacings given by

$$
H(\delta,\lambda) = \frac{1}{n+1}\sum_{i=1}^{n+1}\log D_i(\delta,\lambda).
$$

Moreover, the MPSE can be obtained by solving the following nonlinear expression

$$
\frac{1}{n+1}\sum_{i=1}^{n+1}\frac{1}{D_i(\delta,\lambda)}\left[\Delta_s(x_{(i)}|\delta,\lambda)-\Delta_s(x_{(i-1)}|\delta,\lambda)\right]=0, \quad s=1,2,
$$

where $\Delta_1(\cdot|\delta,\lambda)$ and $\Delta_2(\cdot|\delta,\lambda)$ are defined in Equation (21) and Equation (22), respectively.

4.4. Cramér-Von Mises Estimation Approach

The CVME of the WS-Weibull parameters is obtained by minimizing

$$C(\delta, \lambda) = -\frac{1}{12n} + \sum_{i=1}^{n} \left[F(x_i|\delta, \lambda) - \frac{2i-1}{2n} \right]^2,$$

with respect to δ and λ. Moreover, the CVME can be numerically obtained by solving the following non-linear equation

$$\sum_{i=1}^{n} \left[F(x_i|\delta, \lambda) - \frac{2i-1}{2n} \right] \Delta_s(x_i|\delta, \lambda) = 0, \quad s = 1, 2,$$

where $\Delta_1(\cdot|\delta, \lambda)$ and $\Delta_2(\cdot|\delta, \lambda)$ are, respectively, presented in Equations (21) and (22).

4.5. Anderson–Darling and Right-Tail Anderson-Darling

Suppose that $x_{(1)}, x_{(2)}, \ldots, x_{(n)}$ is the ordered random sample from $F(x|\delta, \lambda)$ of the WS-Weibull model. The ADE of the WS-Weibull parameters can be obtained by minimizing

$$A(\delta, \lambda) = -n - \frac{1}{n} \sum_{i=1}^{n} (2i-1)[\log F(x_i|\delta, \lambda) + \log S(x_i|\delta, \lambda)],$$

or by solving the non-linear equation

$$\sum_{i=1}^{n} (2i-1) \left[\frac{\Delta_s(x_i)}{F(x_i|\delta, \lambda)} - \frac{\Delta_i(x_{n+1-i})}{S(x_{n+1-i}|\delta, \lambda)} \right] = 0, \quad s = 1, 2,$$

Moreover, the RADEs of the WS-Weibull parameters can be obtained by minimizing

$$R(\delta, \lambda) = \frac{n}{2} - 2 \sum_{i=1}^{n} F(x_{i:n}|\delta, \lambda) - \frac{1}{n} \sum_{i=1}^{n} (2i-1) \log S(x_{n+1-i:n}|\delta, \lambda),$$

with respect to δ and λ, which are equivalent by solving the non-linear equations

$$-2 \sum_{i=1}^{n} \Delta_s(x_{i:n}|\delta, \lambda) + \frac{1}{n} \sum_{i=1}^{n} (2i-1) \frac{\Delta_s(x_{n+1-i:n}|\delta, \lambda)}{S(x_{n+1-i:n}|\delta, \lambda)} = 0, \quad s = 1, 2,$$

where $\Delta_1(\cdot|\delta, \lambda)$ and $\Delta_2(\cdot|\delta, \lambda)$ are presented in Equation (21) and Equation (22), respectively.

4.6. Percentile

From (8), the PCE of the parameters of WS-Weibull model can be obtained by minimizing the following function

$$P(p|\delta, \lambda) = \sum_{i=1}^{n} \left[x_{(i)} - \left(-\frac{1}{\lambda} \log \left[1 - \frac{2}{\pi} \sin^{-1}(1 - W_{-1}((1-p)e)) \right] \right)^{1/\delta} \right]^2,$$

with respect to δ and λ, where $0 < p < 1$.

4.7. Simulation Study

In order to explore the performances of the estimators of the WS-Weibull distribution, we consider some detailed simulation studies. The performances of the estimators are judged by considering several statistical tools. These tools include

- The absolute value of biases given by

$$|\text{Bias}(\widehat{\boldsymbol{\vartheta}})| = \frac{1}{N} \sum_{i=1}^{N} |\widehat{\boldsymbol{\vartheta}} - \boldsymbol{\vartheta}|.$$

- The mean square error of the estimates given by

$$MSE\left(\widehat{\boldsymbol{\vartheta}}\right) = \frac{1}{N}\sum_{i=1}^{N}(\widehat{\boldsymbol{\vartheta}} - \boldsymbol{\vartheta})^2.$$

- The mean relative estimates

$$MRE = \left(\widehat{\boldsymbol{\vartheta}}\right) = \frac{1}{N}\sum_{i=1}^{N}|\widehat{\boldsymbol{\vartheta}} - \boldsymbol{\vartheta}|/\boldsymbol{\vartheta}.$$

The values of the estimators are calculated for different samples of sizes, say $n = \{30, 80, 120, 200, 350\}$, taken from the WS-Weibull model. We use R codes throughout the simulations with the nlminb function within the stats package [27].

The simulation studies are carried out for the following parameter combinations: $\delta = \{0.45, 0.75, 1.50, 4.00\}$ and $\lambda = \{0.50, 1.00, 1.75, 3.00\}$. For each setting, the process is repeated $N = 5000$ times and the average values of $|Bias|$, MSE, and MRE for δ and λ are obtained. To save space, four out of sixteen simulated outcomes are reported in Tables 5–8. The numbers in each row have superscripts giving the ranks of the estimates of all methods, and the $\sum Ranks$ is the partial sum of the ranks. Furthermore, Figures 3–6 display the heatmaps of the $|Bias|$, MSE, and MRE for the δ and λ of the simulation results.

Table 9 gives the partial and overall ranks of the estimates, thus indicating that the MPSEs outperform all other estimates for the WS-Weibull model distribution, with an overall score of 117.5.

Table 5. Simulation results for $\boldsymbol{\vartheta} = (\delta = 0.45, \lambda = 0.50)^{\mathsf{T}}$.

n	Est.	Est. Par.	WLSE	OLSE	MLE	MPSE	CVME	ADE	RADE	PCE
30	$|BIAS|$	$\hat{\delta}$	$0.05995^{\{4\}}$	$0.06450^{\{6\}}$	$0.05682^{\{3\}}$	$0.05619^{\{1\}}$	$0.06912^{\{7\}}$	$0.05653^{\{2\}}$	$0.06200^{\{5\}}$	$0.13974^{\{8\}}$
		$\hat{\lambda}$	$0.08844^{\{4\}}$	$0.09183^{\{6\}}$	$0.08879^{\{5\}}$	$0.07678^{\{1\}}$	$0.10129^{\{7\}}$	$0.08676^{\{2\}}$	$0.08707^{\{3\}}$	$0.12877^{\{8\}}$
	MSE	$\hat{\delta}$	$0.00602^{\{4\}}$	$0.00688^{\{6\}}$	$0.00560^{\{3\}}$	$0.00472^{\{1\}}$	$0.00846^{\{7\}}$	$0.00533^{\{2\}}$	$0.00660^{\{5\}}$	$0.02904^{\{8\}}$
		$\hat{\lambda}$	$0.01418^{\{5\}}$	$0.01533^{\{6\}}$	$0.01395^{\{4\}}$	$0.00947^{\{1\}}$	$0.01996^{\{7\}}$	$0.01316^{\{2\}}$	$0.01324^{\{3\}}$	$0.02630^{\{8\}}$
	MRE	$\hat{\delta}$	$0.13322^{\{4\}}$	$0.14334^{\{6\}}$	$0.12627^{\{3\}}$	$0.12487^{\{1\}}$	$0.15361^{\{7\}}$	$0.12562^{\{2\}}$	$0.13777^{\{5\}}$	$0.31052^{\{8\}}$
		$\hat{\lambda}$	$0.17688^{\{4\}}$	$0.18366^{\{6\}}$	$0.17758^{\{5\}}$	$0.15356^{\{1\}}$	$0.20259^{\{7\}}$	$0.17352^{\{2\}}$	$0.17415^{\{3\}}$	$0.25754^{\{8\}}$
	$\sum Ranks$		$25^{\{5\}}$	$36^{\{6\}}$	$23^{\{3\}}$	$6^{\{1\}}$	$42^{\{7\}}$	$12^{\{2\}}$	$24^{\{4\}}$	$48^{\{8\}}$
80	$|BIAS|$	$\hat{\delta}$	$0.03464^{\{4\}}$	$0.03822^{\{6\}}$	$0.03195^{\{1\}}$	$0.03310^{\{2\}}$	$0.03910^{\{7\}}$	$0.03377^{\{3\}}$	$0.03631^{\{5\}}$	$0.10987^{\{8\}}$
		$\hat{\lambda}$	$0.05339^{\{5\}}$	$0.05558^{\{6\}}$	$0.05247^{\{2\}}$	$0.04897^{\{1\}}$	$0.05771^{\{7\}}$	$0.05269^{\{4\}}$	$0.05253^{\{3\}}$	$0.11998^{\{8\}}$
	MSE	$\hat{\delta}$	$0.00192^{\{4\}}$	$0.00232^{\{6\}}$	$0.00165^{\{1\}}$	$0.00166^{\{2\}}$	$0.00249^{\{7\}}$	$0.00182^{\{3\}}$	$0.00212^{\{5\}}$	$0.01895^{\{8\}}$
		$\hat{\lambda}$	$0.00492^{\{5\}}$	$0.00541^{\{6\}}$	$0.00457^{\{2\}}$	$0.00378^{\{1\}}$	$0.00598^{\{7\}}$	$0.00468^{\{4\}}$	$0.00460^{\{3\}}$	$0.02945^{\{8\}}$
	MRE	$\hat{\delta}$	$0.07698^{\{4\}}$	$0.08494^{\{6\}}$	$0.07100^{\{1\}}$	$0.07355^{\{2\}}$	$0.08688^{\{7\}}$	$0.07504^{\{3\}}$	$0.08068^{\{5\}}$	$0.24415^{\{8\}}$
		$\hat{\lambda}$	$0.10679^{\{5\}}$	$0.11117^{\{6\}}$	$0.10493^{\{2\}}$	$0.09794^{\{1\}}$	$0.11542^{\{7\}}$	$0.10538^{\{4\}}$	$0.10505^{\{3\}}$	$0.23997^{\{8\}}$
	$\sum Ranks$		$27^{\{5\}}$	$36^{\{6\}}$	$9^{\{1.5\}}$	$9^{\{1.5\}}$	$42^{\{7\}}$	$21^{\{3\}}$	$24^{\{4\}}$	$48^{\{8\}}$
120	$|BIAS|$	$\hat{\delta}$	$0.02861^{\{4\}}$	$0.03150^{\{6\}}$	$0.02625^{\{1\}}$	$0.02709^{\{2\}}$	$0.03195^{\{7\}}$	$0.02796^{\{3\}}$	$0.02994^{\{5\}}$	$0.09873^{\{8\}}$
		$\hat{\lambda}$	$0.04350^{\{5\}}$	$0.04567^{\{6\}}$	$0.04224^{\{2\}}$	$0.04037^{\{1\}}$	$0.04672^{\{7\}}$	$0.04320^{\{4\}}$	$0.04294^{\{3\}}$	$0.11737^{\{8\}}$
	MSE	$\hat{\delta}$	$0.00131^{\{4\}}$	$0.00158^{\{6\}}$	$0.00112^{\{1\}}$	$0.00113^{\{2\}}$	$0.00165^{\{7\}}$	$0.00124^{\{3\}}$	$0.00145^{\{5\}}$	$0.01581^{\{8\}}$
		$\hat{\lambda}$	$0.00304^{\{5\}}$	$0.00333^{\{6\}}$	$0.00288^{\{2\}}$	$0.00255^{\{1\}}$	$0.00354^{\{7\}}$	$0.00297^{\{4\}}$	$0.00296^{\{3\}}$	$0.03116^{\{8\}}$
	MRE	$\hat{\delta}$	$0.06358^{\{4\}}$	$0.06999^{\{6\}}$	$0.05834^{\{1\}}$	$0.06019^{\{2\}}$	$0.07099^{\{7\}}$	$0.06212^{\{3\}}$	$0.06653^{\{5\}}$	$0.21941^{\{8\}}$
		$\hat{\lambda}$	$0.08699^{\{5\}}$	$0.09135^{\{6\}}$	$0.08447^{\{2\}}$	$0.08073^{\{1\}}$	$0.09345^{\{7\}}$	$0.08639^{\{4\}}$	$0.08588^{\{3\}}$	$0.23474^{\{8\}}$
	$\sum Ranks$		$27^{\{5\}}$	$36^{\{6\}}$	$9^{\{1.5\}}$	$9^{\{1.5\}}$	$42^{\{7\}}$	$21^{\{3\}}$	$24^{\{4\}}$	$48^{\{8\}}$

Table 5. *Cont.*

n	Est.	Est. Par.	WLSE	OLSE	MLE	MPSE	CVME	ADE	RADE	PCE
200	$\|BIAS\|$	$\hat{\delta}$	$0.02157^{\{4\}}$	$0.02409^{\{6\}}$	$0.01990^{\{1\}}$	$0.02058^{\{2\}}$	$0.02430^{\{7\}}$	$0.02128^{\{3\}}$	$0.02262^{\{5\}}$	$0.08542^{\{8\}}$
		$\hat{\lambda}$	$0.03250^{\{5\}}$	$0.03426^{\{6\}}$	$0.03147^{\{2\}}$	$0.03055^{\{1\}}$	$0.03475^{\{7\}}$	$0.03224^{\{4\}}$	$0.03205^{\{3\}}$	$0.10781^{\{8\}}$
	MSE	$\hat{\delta}$	$0.00073^{\{4\}}$	$0.00091^{\{6\}}$	$0.00062^{\{1\}}$	$0.00065^{\{2\}}$	$0.00094^{\{7\}}$	$0.00071^{\{3\}}$	$0.00081^{\{5\}}$	$0.01231^{\{8\}}$
		$\hat{\lambda}$	$0.00168^{\{5\}}$	$0.00187^{\{6\}}$	$0.00158^{\{2\}}$	$0.00146^{\{1\}}$	$0.00194^{\{7\}}$	$0.00165^{\{4\}}$	$0.00163^{\{3\}}$	$0.02986^{\{8\}}$
	MRE	$\hat{\delta}$	$0.04793^{\{4\}}$	$0.05353^{\{6\}}$	$0.04422^{\{1\}}$	$0.04574^{\{2\}}$	$0.05399^{\{7\}}$	$0.04728^{\{3\}}$	$0.05027^{\{5\}}$	$0.18983^{\{8\}}$
		$\hat{\lambda}$	$0.06501^{\{5\}}$	$0.06852^{\{6\}}$	$0.06294^{\{2\}}$	$0.06111^{\{1\}}$	$0.06950^{\{7\}}$	$0.06449^{\{4\}}$	$0.06410^{\{3\}}$	$0.21563^{\{8\}}$
	$\sum Ranks$		$27^{\{5\}}$	$36^{\{6\}}$	$9^{\{1.5\}}$	$9^{\{1.5\}}$	$42^{\{7\}}$	$21^{\{3\}}$	$24^{\{4\}}$	$48^{\{8\}}$
350	$\|BIAS\|$	$\hat{\delta}$	$0.01625^{\{4\}}$	$0.01819^{\{6\}}$	$0.01503^{\{1\}}$	$0.01551^{\{2\}}$	$0.01826^{\{7\}}$	$0.01614^{\{3\}}$	$0.01703^{\{5\}}$	$0.07426^{\{8\}}$
		$\hat{\lambda}$	$0.02426^{\{5\}}$	$0.02557^{\{6\}}$	$0.02364^{\{2\}}$	$0.02330^{\{1\}}$	$0.02577^{\{7\}}$	$0.02418^{\{4\}}$	$0.02399^{\{3\}}$	$0.09992^{\{8\}}$
	MSE	$\hat{\delta}$	$0.00042^{\{4\}}$	$0.00052^{\{6\}}$	$0.00036^{\{1\}}$	$0.00038^{\{2\}}$	$0.00053^{\{7\}}$	$0.00041^{\{3\}}$	$0.00046^{\{5\}}$	$0.00954^{\{8\}}$
		$\hat{\lambda}$	$0.00096^{\{5\}}$	$0.00106^{\{6\}}$	$0.00091^{\{2\}}$	$0.00086^{\{1\}}$	$0.00109^{\{7\}}$	$0.00095^{\{4\}}$	$0.00094^{\{3\}}$	$0.02750^{\{8\}}$
	MRE	$\hat{\delta}$	$0.03612^{\{4\}}$	$0.04042^{\{6\}}$	$0.03341^{\{1\}}$	$0.03447^{\{2\}}$	$0.04059^{\{7\}}$	$0.03587^{\{3\}}$	$0.03784^{\{5\}}$	$0.16503^{\{8\}}$
		$\hat{\lambda}$	$0.04853^{\{5\}}$	$0.05114^{\{6\}}$	$0.04729^{\{2\}}$	$0.04660^{\{1\}}$	$0.05154^{\{7\}}$	$0.04836^{\{4\}}$	$0.04797^{\{3\}}$	$0.19983^{\{8\}}$
	$\sum Ranks$		$27^{\{5\}}$	$36^{\{6\}}$	$9^{\{1.5\}}$	$9^{\{1.5\}}$	$42^{\{7\}}$	$21^{\{3\}}$	$24^{\{4\}}$	$48^{\{8\}}$

Table 6. Simulation results for $\boldsymbol{\vartheta} = (\delta = 0.45, \lambda = 3.00)^{\mathsf{T}}$.

n	Est.	Est. Par.	WLSE	OLSE	MLE	MPSE	CVME	ADE	RADE	PCE
30	$\|BIAS\|$	$\hat{\delta}$	$0.05971^{\{4\}}$	$0.06420^{\{6\}}$	$0.05651^{\{3\}}$	$0.05581^{\{1\}}$	$0.06864^{\{7\}}$	$0.05621^{\{2\}}$	$0.06158^{\{5\}}$	$0.13667^{\{8\}}$
		$\hat{\lambda}$	$1.12196^{\{5\}}$	$1.21709^{\{6\}}$	$1.08373^{\{3\}}$	$0.84246^{\{1\}}$	$1.51324^{\{7\}}$	$1.01079^{\{2\}}$	$1.11567^{\{4\}}$	$1.63339^{\{8\}}$
	MSE	$\hat{\delta}$	$0.00609^{\{4\}}$	$0.00693^{\{6\}}$	$0.00556^{\{3\}}$	$0.00466^{\{1\}}$	$0.00850^{\{7\}}$	$0.00525^{\{2\}}$	$0.00658^{\{5\}}$	$0.02832^{\{8\}}$
		$\hat{\lambda}$	$4.22063^{\{5\}}$	$5.49202^{\{6\}}$	$3.15053^{\{3\}}$	$1.31291^{\{1\}}$	$10.36952^{\{8\}}$	$2.49643^{\{2\}}$	$4.12599^{\{4\}}$	$9.25795^{\{7\}}$
	MRE	$\hat{\delta}$	$0.13270^{\{4\}}$	$0.14267^{\{6\}}$	$0.12557^{\{3\}}$	$0.12401^{\{1\}}$	$0.15252^{\{7\}}$	$0.12491^{\{2\}}$	$0.13685^{\{5\}}$	$0.30370^{\{8\}}$
		$\hat{\lambda}$	$0.37399^{\{5\}}$	$0.40570^{\{6\}}$	$0.36124^{\{3\}}$	$0.28082^{\{1\}}$	$0.50441^{\{7\}}$	$0.33693^{\{2\}}$	$0.37189^{\{4\}}$	$0.54446^{\{8\}}$
	$\sum Ranks$		$27^{\{4.5\}}$	$36^{\{6\}}$	$18^{\{3\}}$	$6^{\{1\}}$	$43^{\{7\}}$	$12^{\{2\}}$	$27^{\{4.5\}}$	$47^{\{8\}}$
80	$\|BIAS\|$	$\hat{\delta}$	$0.03402^{\{4\}}$	$0.03796^{\{6\}}$	$0.03160^{\{1\}}$	$0.03287^{\{2\}}$	$0.03885^{\{7\}}$	$0.03293^{\{3\}}$	$0.03535^{\{5\}}$	$0.11267^{\{8\}}$
		$\hat{\lambda}$	$0.57172^{\{4\}}$	$0.64569^{\{6\}}$	$0.53441^{\{2\}}$	$0.48778^{\{1\}}$	$0.69673^{\{7\}}$	$0.54880^{\{3\}}$	$0.57223^{\{5\}}$	$0.79479^{\{8\}}$
	MSE	$\hat{\delta}$	$0.00188^{\{4\}}$	$0.00232^{\{6\}}$	$0.00163^{\{1.5\}}$	$0.00163^{\{1.5\}}$	$0.00251^{\{7\}}$	$0.00176^{\{3\}}$	$0.00204^{\{5\}}$	$0.02171^{\{8\}}$
		$\hat{\lambda}$	$0.61772^{\{5\}}$	$0.80634^{\{6\}}$	$0.51857^{\{2\}}$	$0.36839^{\{1\}}$	$1.00380^{\{7\}}$	$0.54497^{\{3\}}$	$0.60290^{\{4\}}$	$1.00973^{\{8\}}$
	MRE	$\hat{\delta}$	$0.07559^{\{4\}}$	$0.08435^{\{6\}}$	$0.07021^{\{1\}}$	$0.07304^{\{2\}}$	$0.08634^{\{7\}}$	$0.07318^{\{3\}}$	$0.07855^{\{5\}}$	$0.25038^{\{8\}}$
		$\hat{\lambda}$	$0.19057^{\{4\}}$	$0.21523^{\{6\}}$	$0.17814^{\{2\}}$	$0.16259^{\{1\}}$	$0.23224^{\{7\}}$	$0.18293^{\{3\}}$	$0.19074^{\{5\}}$	$0.26493^{\{8\}}$
	$\sum Ranks$		$25^{\{4\}}$	$36^{\{6\}}$	$9.5^{\{2\}}$	$8.5^{\{1\}}$	$42^{\{7\}}$	$18^{\{3\}}$	$29^{\{5\}}$	$48^{\{8\}}$
120	$\|BIAS\|$	$\hat{\delta}$	$0.02747^{\{4\}}$	$0.03039^{\{6\}}$	$0.02559^{\{1\}}$	$0.02655^{\{2\}}$	$0.03090^{\{7\}}$	$0.02686^{\{3\}}$	$0.02865^{\{5\}}$	$0.10426^{\{8\}}$
		$\hat{\lambda}$	$0.44990^{\{4\}}$	$0.50301^{\{6\}}$	$0.41951^{\{2\}}$	$0.39811^{\{1\}}$	$0.52717^{\{7\}}$	$0.43823^{\{3\}}$	$0.45485^{\{5\}}$	$0.70458^{\{8\}}$
	MSE	$\hat{\delta}$	$0.00121^{\{4\}}$	$0.00147^{\{6\}}$	$0.00107^{\{1\}}$	$0.00108^{\{2\}}$	$0.00155^{\{7\}}$	$0.00116^{\{3\}}$	$0.00134^{\{5\}}$	$0.01861^{\{8\}}$
		$\hat{\lambda}$	$0.36433^{\{4\}}$	$0.45494^{\{6\}}$	$0.31850^{\{2\}}$	$0.25459^{\{1\}}$	$0.52517^{\{7\}}$	$0.34239^{\{3\}}$	$0.37420^{\{5\}}$	$0.76800^{\{8\}}$
	MRE	$\hat{\delta}$	$0.06105^{\{4\}}$	$0.06754^{\{6\}}$	$0.05686^{\{1\}}$	$0.05900^{\{2\}}$	$0.06866^{\{7\}}$	$0.05969^{\{3\}}$	$0.06367^{\{5\}}$	$0.23169^{\{8\}}$
		$\hat{\lambda}$	$0.14997^{\{4\}}$	$0.16767^{\{6\}}$	$0.13984^{\{2\}}$	$0.13270^{\{1\}}$	$0.17572^{\{7\}}$	$0.14608^{\{3\}}$	$0.15162^{\{5\}}$	$0.23486^{\{8\}}$
	$\sum Ranks$		$24^{\{4\}}$	$36^{\{6\}}$	$9^{\{1.5\}}$	$9^{\{1.5\}}$	$42^{\{7\}}$	$18^{\{3\}}$	$30^{\{5\}}$	$48^{\{8\}}$
200	$\|BIAS\|$	$\hat{\delta}$	$0.02204^{\{4\}}$	$0.02465^{\{6\}}$	$0.02002^{\{1\}}$	$0.02099^{\{2\}}$	$0.02480^{\{7\}}$	$0.02159^{\{3\}}$	$0.02250^{\{5\}}$	$0.08845^{\{8\}}$
		$\hat{\lambda}$	$0.35292^{\{5\}}$	$0.39916^{\{6\}}$	$0.31828^{\{2\}}$	$0.31005^{\{1\}}$	$0.41017^{\{7\}}$	$0.34345^{\{3\}}$	$0.34659^{\{4\}}$	$0.57534^{\{8\}}$
	MSE	$\hat{\delta}$	$0.00077^{\{4\}}$	$0.00096^{\{6\}}$	$0.00064^{\{1\}}$	$0.00067^{\{2\}}$	$0.00099^{\{7\}}$	$0.00074^{\{3\}}$	$0.00082^{\{5\}}$	$0.01333^{\{8\}}$
		$\hat{\lambda}$	$0.21230^{\{5\}}$	$0.27196^{\{6\}}$	$0.17276^{\{2\}}$	$0.15367^{\{1\}}$	$0.29665^{\{7\}}$	$0.19999^{\{3\}}$	$0.20515^{\{4\}}$	$0.49874^{\{8\}}$
	MRE	$\hat{\delta}$	$0.04898^{\{4\}}$	$0.05478^{\{6\}}$	$0.04449^{\{1\}}$	$0.04665^{\{2\}}$	$0.05511^{\{7\}}$	$0.04798^{\{3\}}$	$0.05001^{\{5\}}$	$0.19655^{\{8\}}$
		$\hat{\lambda}$	$0.11764^{\{5\}}$	$0.13305^{\{6\}}$	$0.10609^{\{2\}}$	$0.10335^{\{1\}}$	$0.13672^{\{7\}}$	$0.11448^{\{3\}}$	$0.11553^{\{4\}}$	$0.19178^{\{8\}}$
	$\sum Ranks$		$27^{\{4.5\}}$	$36^{\{6\}}$	$9^{\{1.5\}}$	$9^{\{1.5\}}$	$42^{\{7\}}$	$18^{\{3\}}$	$27^{\{4.5\}}$	$48^{\{8\}}$
350	$\|BIAS\|$	$\hat{\delta}$	$0.01603^{\{4\}}$	$0.01790^{\{6\}}$	$0.01472^{\{1\}}$	$0.01516^{\{2\}}$	$0.01798^{\{7\}}$	$0.01583^{\{3\}}$	$0.01670^{\{5\}}$	$0.07556^{\{8\}}$
		$\hat{\lambda}$	$0.25736^{\{5\}}$	$0.29045^{\{6\}}$	$0.23334^{\{2\}}$	$0.22047^{\{1\}}$	$0.29502^{\{7\}}$	$0.25314^{\{3\}}$	$0.25613^{\{4\}}$	$0.45532^{\{8\}}$
	MSE	$\hat{\delta}$	$0.00041^{\{4\}}$	$0.00051^{\{6\}}$	$0.00034^{\{1\}}$	$0.00036^{\{2\}}$	$0.00052^{\{7\}}$	$0.00040^{\{3\}}$	$0.00044^{\{5\}}$	$0.00980^{\{8\}}$
		$\hat{\lambda}$	$0.10852^{\{5\}}$	$0.13908^{\{6\}}$	$0.08890^{\{2\}}$	$0.08355^{\{1\}}$	$0.14606^{\{7\}}$	$0.10417^{\{3\}}$	$0.10831^{\{4\}}$	$0.30891^{\{8\}}$
	MRE	$\hat{\delta}$	$0.03563^{\{4\}}$	$0.03978^{\{6\}}$	$0.03271^{\{1\}}$	$0.03369^{\{2\}}$	$0.03995^{\{7\}}$	$0.03517^{\{3\}}$	$0.03712^{\{5\}}$	$0.16791^{\{8\}}$
		$\hat{\lambda}$	$0.08579^{\{5\}}$	$0.09682^{\{6\}}$	$0.07778^{\{2\}}$	$0.07349^{\{1\}}$	$0.09834^{\{7\}}$	$0.08438^{\{3\}}$	$0.08538^{\{4\}}$	$0.15177^{\{8\}}$
	$\sum Ranks$		$27^{\{4.5\}}$	$36^{\{6\}}$	$9^{\{1.5\}}$	$9^{\{1.5\}}$	$42^{\{7\}}$	$18^{\{3\}}$	$27^{\{4.5\}}$	$48^{\{8\}}$

Table 7. Simulation results for $\boldsymbol{\vartheta} = (\delta = 0.75, \lambda = 0.50)^{\mathsf{T}}$.

n	Est.	Est. Par.	WLSE	OLSE	MLE	MPSE	CVME	ADE	RADE	PCE
30	|BIAS|	$\hat{\delta}$	$0.09871^{\{4\}}$	$0.10640^{\{6\}}$	$0.09417^{\{3\}}$	$0.09199^{\{1\}}$	$0.11374^{\{7\}}$	$0.09328^{\{2\}}$	$0.10185^{\{5\}}$	$0.16592^{\{8\}}$
		$\hat{\lambda}$	$0.09056^{\{4\}}$	$0.09400^{\{7\}}$	$0.09115^{\{5\}}$	$0.07839^{\{1\}}$	$0.10412^{\{8\}}$	$0.08816^{\{2\}}$	$0.08853^{\{3\}}$	$0.09283^{\{6\}}$
	MSE	$\hat{\delta}$	$0.01668^{\{4\}}$	$0.01937^{\{6\}}$	$0.01524^{\{3\}}$	$0.01283^{\{1\}}$	$0.02362^{\{7\}}$	$0.01442^{\{2\}}$	$0.01768^{\{5\}}$	$0.04375^{\{8\}}$
		$\hat{\lambda}$	$0.01595^{\{6\}}$	$0.01825^{\{7\}}$	$0.01529^{\{5\}}$	$0.01017^{\{1\}}$	$0.02430^{\{8\}}$	$0.01422^{\{2\}}$	$0.01442^{\{3\}}$	$0.01468^{\{4\}}$
	MRE	$\hat{\delta}$	$0.13161^{\{4\}}$	$0.14186^{\{6\}}$	$0.12556^{\{3\}}$	$0.12265^{\{1\}}$	$0.15166^{\{7\}}$	$0.12437^{\{2\}}$	$0.13580^{\{5\}}$	$0.22122^{\{8\}}$
		$\hat{\lambda}$	$0.18112^{\{4\}}$	$0.18800^{\{7\}}$	$0.18230^{\{5\}}$	$0.15677^{\{1\}}$	$0.20825^{\{8\}}$	$0.17631^{\{2\}}$	$0.17705^{\{3\}}$	$0.18565^{\{6\}}$
	$\sum Ranks$		$26^{\{5\}}$	$39^{\{6\}}$	$24^{\{3.5\}}$	$6^{\{1\}}$	$45^{\{8\}}$	$12^{\{2\}}$	$24^{\{3.5\}}$	$40^{\{7\}}$
80	|BIAS|	$\hat{\delta}$	$0.05830^{\{4\}}$	$0.06451^{\{6\}}$	$0.05363^{\{1\}}$	$0.05486^{\{2\}}$	$0.06619^{\{7\}}$	$0.05670^{\{3\}}$	$0.06013^{\{5\}}$	$0.11911^{\{8\}}$
		$\hat{\lambda}$	$0.05319^{\{5\}}$	$0.05535^{\{6\}}$	$0.05218^{\{2\}}$	$0.04890^{\{1\}}$	$0.05732^{\{7\}}$	$0.05259^{\{3.5\}}$	$0.05259^{\{3.5\}}$	$0.06567^{\{8\}}$
	MSE	$\hat{\delta}$	$0.00544^{\{4\}}$	$0.00663^{\{6\}}$	$0.00471^{\{2\}}$	$0.00462^{\{1\}}$	$0.00719^{\{7\}}$	$0.00513^{\{3\}}$	$0.00591^{\{5\}}$	$0.02320^{\{8\}}$
		$\hat{\lambda}$	$0.00468^{\{5\}}$	$0.00510^{\{6\}}$	$0.00449^{\{2\}}$	$0.00378^{\{1\}}$	$0.00560^{\{7\}}$	$0.00455^{\{3\}}$	$0.00456^{\{4\}}$	$0.00782^{\{8\}}$
	MRE	$\hat{\delta}$	$0.07774^{\{4\}}$	$0.08602^{\{6\}}$	$0.07150^{\{1\}}$	$0.07315^{\{2\}}$	$0.08825^{\{7\}}$	$0.07561^{\{3\}}$	$0.08017^{\{5\}}$	$0.15881^{\{8\}}$
		$\hat{\lambda}$	$0.10637^{\{5\}}$	$0.11070^{\{6\}}$	$0.10437^{\{2\}}$	$0.09780^{\{1\}}$	$0.11464^{\{7\}}$	$0.10519^{\{4\}}$	$0.10517^{\{3\}}$	$0.13135^{\{8\}}$
	$\sum Ranks$		$27^{\{5\}}$	$36^{\{6\}}$	$10^{\{2\}}$	$8^{\{1\}}$	$42^{\{7\}}$	$19.5^{\{3\}}$	$25.5^{\{4\}}$	$48^{\{8\}}$
120	|BIAS|	$\hat{\delta}$	$0.04696^{\{4\}}$	$0.05194^{\{6\}}$	$0.04361^{\{1\}}$	$0.04479^{\{2\}}$	$0.05282^{\{7\}}$	$0.04612^{\{3\}}$	$0.04939^{\{5\}}$	$0.10186^{\{8\}}$
		$\hat{\lambda}$	$0.04386^{\{5\}}$	$0.04606^{\{6\}}$	$0.04274^{\{2\}}$	$0.04059^{\{1\}}$	$0.04722^{\{7\}}$	$0.04351^{\{4\}}$	$0.04341^{\{3\}}$	$0.05651^{\{8\}}$
	MSE	$\hat{\delta}$	$0.00349^{\{4\}}$	$0.00428^{\{6\}}$	$0.00301^{\{1\}}$	$0.00304^{\{2\}}$	$0.00451^{\{7\}}$	$0.00334^{\{3\}}$	$0.00387^{\{5\}}$	$0.01717^{\{8\}}$
		$\hat{\lambda}$	$0.00310^{\{5\}}$	$0.00340^{\{6\}}$	$0.00299^{\{2\}}$	$0.00261^{\{1\}}$	$0.00363^{\{7\}}$	$0.00303^{\{3.5\}}$	$0.00303^{\{3.5\}}$	$0.00589^{\{8\}}$
	MRE	$\hat{\delta}$	$0.06262^{\{4\}}$	$0.06925^{\{6\}}$	$0.05814^{\{1\}}$	$0.05973^{\{2\}}$	$0.07043^{\{7\}}$	$0.06149^{\{3\}}$	$0.06586^{\{5\}}$	$0.13582^{\{8\}}$
		$\hat{\lambda}$	$0.08773^{\{5\}}$	$0.09212^{\{6\}}$	$0.08547^{\{2\}}$	$0.08117^{\{1\}}$	$0.09444^{\{7\}}$	$0.08703^{\{4\}}$	$0.08683^{\{3\}}$	$0.11303^{\{8\}}$
	$\sum Ranks$		$27^{\{5\}}$	$36^{\{6\}}$	$9^{\{1.5\}}$	$9^{\{1.5\}}$	$42^{\{7\}}$	$20.5^{\{3\}}$	$24.5^{\{4\}}$	$48^{\{8\}}$
200	|BIAS|	$\hat{\delta}$	$0.03643^{\{4\}}$	$0.04049^{\{6\}}$	$0.03307^{\{1\}}$	$0.03426^{\{2\}}$	$0.04082^{\{7\}}$	$0.03593^{\{3\}}$	$0.03793^{\{5\}}$	$0.08370^{\{8\}}$
		$\hat{\lambda}$	$0.03296^{\{5\}}$	$0.03447^{\{6\}}$	$0.03222^{\{2\}}$	$0.03115^{\{1\}}$	$0.03499^{\{7\}}$	$0.03278^{\{4\}}$	$0.03263^{\{3\}}$	$0.04497^{\{8\}}$
	MSE	$\hat{\delta}$	$0.00209^{\{4\}}$	$0.00258^{\{6\}}$	$0.00176^{\{1\}}$	$0.00180^{\{2\}}$	$0.00266^{\{7\}}$	$0.00203^{\{3\}}$	$0.00230^{\{5\}}$	$0.01152^{\{8\}}$
		$\hat{\lambda}$	$0.00173^{\{5\}}$	$0.00190^{\{6\}}$	$0.00165^{\{2\}}$	$0.00152^{\{1\}}$	$0.00197^{\{7\}}$	$0.00171^{\{4\}}$	$0.00169^{\{3\}}$	$0.00375^{\{8\}}$
	MRE	$\hat{\delta}$	$0.04857^{\{4\}}$	$0.05399^{\{6\}}$	$0.04409^{\{1\}}$	$0.04568^{\{2\}}$	$0.05443^{\{7\}}$	$0.04791^{\{3\}}$	$0.05058^{\{5\}}$	$0.11160^{\{8\}}$
		$\hat{\lambda}$	$0.06592^{\{5\}}$	$0.06895^{\{6\}}$	$0.06445^{\{2\}}$	$0.06230^{\{1\}}$	$0.06999^{\{7\}}$	$0.06557^{\{4\}}$	$0.06525^{\{3\}}$	$0.08995^{\{8\}}$
	$\sum Ranks$		$27^{\{5\}}$	$36^{\{6\}}$	$9^{\{1.5\}}$	$9^{\{1.5\}}$	$42^{\{7\}}$	$21^{\{3\}}$	$24^{\{4\}}$	$48^{\{8\}}$
350	|BIAS|	$\hat{\delta}$	$0.02723^{\{4\}}$	$0.03035^{\{6\}}$	$0.02505^{\{1\}}$	$0.02571^{\{2\}}$	$0.03051^{\{7\}}$	$0.02704^{\{3\}}$	$0.02837^{\{5\}}$	$0.06672^{\{8\}}$
		$\hat{\lambda}$	$0.02468^{\{5\}}$	$0.02597^{\{6\}}$	$0.02395^{\{2\}}$	$0.02366^{\{1\}}$	$0.02613^{\{7\}}$	$0.02460^{\{4\}}$	$0.02448^{\{3\}}$	$0.03502^{\{8\}}$
	MSE	$\hat{\delta}$	$0.00116^{\{4\}}$	$0.00145^{\{6\}}$	$0.00099^{\{1\}}$	$0.00102^{\{2\}}$	$0.00148^{\{7\}}$	$0.00114^{\{3\}}$	$0.00126^{\{5\}}$	$0.00720^{\{8\}}$
		$\hat{\lambda}$	$0.00097^{\{5\}}$	$0.00107^{\{6\}}$	$0.00091^{\{2\}}$	$0.00088^{\{1\}}$	$0.00109^{\{7\}}$	$0.00096^{\{4\}}$	$0.00095^{\{3\}}$	$0.00213^{\{8\}}$
	MRE	$\hat{\delta}$	$0.03631^{\{4\}}$	$0.04046^{\{6\}}$	$0.03340^{\{1\}}$	$0.03428^{\{2\}}$	$0.04068^{\{7\}}$	$0.03606^{\{3\}}$	$0.03783^{\{5\}}$	$0.08897^{\{8\}}$
		$\hat{\lambda}$	$0.04937^{\{5\}}$	$0.05193^{\{6\}}$	$0.04791^{\{2\}}$	$0.04732^{\{1\}}$	$0.05227^{\{7\}}$	$0.04921^{\{4\}}$	$0.04896^{\{3\}}$	$0.07005^{\{8\}}$
	$\sum Ranks$		$27^{\{5\}}$	$36^{\{6\}}$	$9^{\{1.5\}}$	$9^{\{1.5\}}$	$42^{\{7\}}$	$21^{\{3\}}$	$24^{\{4\}}$	$48^{\{8\}}$

Table 8. Simulation results for $\boldsymbol{\vartheta} = (\delta = 4.00, \lambda = 3.00)^{\mathsf{T}}$.

n	Est.	Est. Par.	WLSE	OLSE	MLE	MPSE	CVME	ADE	RADE	PCE
30	|BIAS|	$\hat{\delta}$	$0.52826^{\{5\}}$	$0.57159^{\{7\}}$	$0.49972^{\{3\}}$	$0.49193^{\{2\}}$	$0.61053^{\{8\}}$	$0.50005^{\{4\}}$	$0.55036^{\{6\}}$	$0.47654^{\{1\}}$
		$\hat{\lambda}$	$1.11327^{\{6\}}$	$1.20970^{\{7\}}$	$1.07414^{\{4\}}$	$0.82845^{\{1\}}$	$1.50679^{\{8\}}$	$1.01227^{\{3\}}$	$1.09974^{\{5\}}$	$0.85244^{\{2\}}$
	MSE	$\hat{\delta}$	$0.47263^{\{5\}}$	$0.54656^{\{7\}}$	$0.42643^{\{4\}}$	$0.36760^{\{2\}}$	$0.66271^{\{8\}}$	$0.41285^{\{3\}}$	$0.51336^{\{6\}}$	$0.35080^{\{1\}}$
		$\hat{\lambda}$	$4.47860^{\{6\}}$	$5.30036^{\{7\}}$	$2.98339^{\{4\}}$	$1.22399^{\{1\}}$	$10.16763^{\{8\}}$	$2.43795^{\{3\}}$	$3.46274^{\{5\}}$	$1.44294^{\{2\}}$
	MRE	$\hat{\delta}$	$0.13207^{\{5\}}$	$0.14290^{\{7\}}$	$0.12493^{\{3\}}$	$0.12298^{\{2\}}$	$0.15263^{\{8\}}$	$0.12501^{\{4\}}$	$0.13759^{\{6\}}$	$0.11914^{\{1\}}$
		$\hat{\lambda}$	$0.37109^{\{6\}}$	$0.40323^{\{7\}}$	$0.35805^{\{4\}}$	$0.27615^{\{1\}}$	$0.50226^{\{8\}}$	$0.33742^{\{3\}}$	$0.36658^{\{5\}}$	$0.28415^{\{2\}}$
	$\sum Ranks$		$33^{\{5.5\}}$	$42^{\{7\}}$	$22^{\{4\}}$	$9^{\{1.5\}}$	$48^{\{8\}}$	$20^{\{3\}}$	$33^{\{5.5\}}$	$9^{\{1.5\}}$

Table 8. *Cont.*

n	Est.	Est. Par.	WLSE	OLSE	MLE	MPSE	CVME	ADE	RADE	PCE
80	$\|BIAS\|$	$\hat{\delta}$	$0.31405^{\{5\}}$	$0.34365^{\{7\}}$	$0.29344^{\{2\}}$	$0.29929^{\{3\}}$	$0.35267^{\{8\}}$	$0.30589^{\{4\}}$	$0.32689^{\{6\}}$	$0.28668^{\{1\}}$
		$\hat{\lambda}$	$0.58521^{\{5\}}$	$0.64431^{\{7\}}$	$0.54668^{\{3\}}$	$0.49869^{\{2\}}$	$0.69457^{\{8\}}$	$0.56545^{\{4\}}$	$0.58551^{\{6\}}$	$0.49536^{\{1\}}$
	MSE	$\hat{\delta}$	$0.16033^{\{5\}}$	$0.19008^{\{7\}}$	$0.14142^{\{3\}}$	$0.13794^{\{2\}}$	$0.20551^{\{8\}}$	$0.15127^{\{4\}}$	$0.17565^{\{6\}}$	$0.12673^{\{1\}}$
		$\hat{\lambda}$	$0.65356^{\{5\}}$	$0.80065^{\{7\}}$	$0.56111^{\{3\}}$	$0.38873^{\{1\}}$	$0.99591^{\{8\}}$	$0.58436^{\{4\}}$	$0.65407^{\{6\}}$	$0.40210^{\{2\}}$
	MRE	$\hat{\delta}$	$0.07851^{\{5\}}$	$0.08591^{\{7\}}$	$0.07336^{\{2\}}$	$0.07482^{\{3\}}$	$0.08817^{\{8\}}$	$0.07647^{\{4\}}$	$0.08172^{\{6\}}$	$0.07167^{\{1\}}$
		$\hat{\lambda}$	$0.19507^{\{5\}}$	$0.21477^{\{7\}}$	$0.18223^{\{3\}}$	$0.16623^{\{2\}}$	$0.23152^{\{8\}}$	$0.18848^{\{4\}}$	$0.19517^{\{6\}}$	$0.16512^{\{1\}}$
	$\sum Ranks$		$30^{\{5\}}$	$42^{\{7\}}$	$16^{\{3\}}$	$13^{\{2\}}$	$48^{\{8\}}$	$24^{\{4\}}$	$36^{\{6\}}$	$7^{\{1\}}$
120	$\|BIAS\|$	$\hat{\delta}$	$0.24785^{\{5\}}$	$0.27563^{\{7\}}$	$0.22778^{\{1\}}$	$0.23683^{\{3\}}$	$0.27983^{\{8\}}$	$0.24208^{\{4\}}$	$0.25873^{\{6\}}$	$0.23191^{\{2\}}$
		$\hat{\lambda}$	$0.46276^{\{6\}}$	$0.51714^{\{7\}}$	$0.42345^{\{3\}}$	$0.40160^{\{1\}}$	$0.54292^{\{8\}}$	$0.45070^{\{4\}}$	$0.45972^{\{5\}}$	$0.40345^{\{2\}}$
	MSE	$\hat{\delta}$	$0.09895^{\{5\}}$	$0.12081^{\{7\}}$	$0.08373^{\{2\}}$	$0.08601^{\{3\}}$	$0.12657^{\{8\}}$	$0.09418^{\{4\}}$	$0.10699^{\{6\}}$	$0.08253^{\{1\}}$
		$\hat{\lambda}$	$0.38541^{\{6\}}$	$0.47566^{\{7\}}$	$0.32147^{\{3\}}$	$0.25482^{\{1\}}$	$0.54743^{\{8\}}$	$0.35719^{\{4\}}$	$0.38073^{\{5\}}$	$0.25766^{\{2\}}$
	MRE	$\hat{\delta}$	$0.06196^{\{5\}}$	$0.06891^{\{7\}}$	$0.05695^{\{1\}}$	$0.05921^{\{3\}}$	$0.06996^{\{8\}}$	$0.06052^{\{4\}}$	$0.06468^{\{6\}}$	$0.05798^{\{2\}}$
		$\hat{\lambda}$	$0.15425^{\{6\}}$	$0.17238^{\{7\}}$	$0.14115^{\{3\}}$	$0.13387^{\{1\}}$	$0.18097^{\{8\}}$	$0.15023^{\{4\}}$	$0.15324^{\{5\}}$	$0.13448^{\{2\}}$
	$\sum Ranks$		$33^{\{5.5\}}$	$42^{\{7\}}$	$13^{\{3\}}$	$12^{\{2\}}$	$48^{\{8\}}$	$24^{\{4\}}$	$33^{\{5.5\}}$	$11^{\{1\}}$
200	$\|BIAS\|$	$\hat{\delta}$	$0.19032^{\{5\}}$	$0.21310^{\{7\}}$	$0.17553^{\{1\}}$	$0.18020^{\{3\}}$	$0.21485^{\{8\}}$	$0.18778^{\{4\}}$	$0.20132^{\{6\}}$	$0.17810^{\{2\}}$
		$\hat{\lambda}$	$0.34904^{\{5\}}$	$0.39646^{\{7\}}$	$0.32026^{\{3\}}$	$0.30712^{\{1\}}$	$0.40727^{\{8\}}$	$0.34387^{\{4\}}$	$0.35187^{\{6\}}$	$0.31010^{\{2\}}$
	MSE	$\hat{\delta}$	$0.05734^{\{5\}}$	$0.07127^{\{7\}}$	$0.04936^{\{1\}}$	$0.05018^{\{3\}}$	$0.07360^{\{8\}}$	$0.05576^{\{4\}}$	$0.06396^{\{6\}}$	$0.04942^{\{2\}}$
		$\hat{\lambda}$	$0.20823^{\{5\}}$	$0.26525^{\{7\}}$	$0.17626^{\{3\}}$	$0.15069^{\{1\}}$	$0.28980^{\{8\}}$	$0.19912^{\{4\}}$	$0.21183^{\{6\}}$	$0.15211^{\{2\}}$
	MRE	$\hat{\delta}$	$0.04758^{\{5\}}$	$0.05327^{\{7\}}$	$0.04388^{\{1\}}$	$0.04505^{\{3\}}$	$0.05371^{\{8\}}$	$0.04694^{\{4\}}$	$0.05033^{\{6\}}$	$0.04453^{\{2\}}$
		$\hat{\lambda}$	$0.11635^{\{5\}}$	$0.13215^{\{7\}}$	$0.10675^{\{3\}}$	$0.10237^{\{1\}}$	$0.13576^{\{8\}}$	$0.11462^{\{4\}}$	$0.11729^{\{6\}}$	$0.10337^{\{2\}}$
	$\sum Ranks$		$30^{\{5\}}$	$42^{\{7\}}$	$12^{\{2\}}$	$12^{\{2\}}$	$48^{\{8\}}$	$24^{\{4\}}$	$36^{\{6\}}$	$12^{\{2\}}$
350	$\|BIAS\|$	$\hat{\delta}$	$0.14365^{\{5\}}$	$0.16163^{\{7\}}$	$0.13133^{\{1\}}$	$0.13467^{\{3\}}$	$0.16271^{\{8\}}$	$0.14229^{\{4\}}$	$0.15007^{\{6\}}$	$0.13357^{\{2\}}$
		$\hat{\lambda}$	$0.26016^{\{6\}}$	$0.29563^{\{7\}}$	$0.23584^{\{3\}}$	$0.22725^{\{1\}}$	$0.30114^{\{8\}}$	$0.25688^{\{4\}}$	$0.25873^{\{5\}}$	$0.23506^{\{2\}}$
	MSE	$\hat{\delta}$	$0.03327^{\{5\}}$	$0.04177^{\{7\}}$	$0.02804^{\{2\}}$	$0.02876^{\{3\}}$	$0.04261^{\{8\}}$	$0.03259^{\{4\}}$	$0.03626^{\{6\}}$	$0.02789^{\{1\}}$
		$\hat{\lambda}$	$0.11087^{\{6\}}$	$0.14275^{\{7\}}$	$0.09219^{\{3\}}$	$0.08504^{\{1\}}$	$0.15033^{\{8\}}$	$0.10750^{\{4\}}$	$0.10999^{\{5\}}$	$0.08680^{\{2\}}$
	MRE	$\hat{\delta}$	$0.03591^{\{5\}}$	$0.04041^{\{7\}}$	$0.03283^{\{1\}}$	$0.03367^{\{3\}}$	$0.04068^{\{8\}}$	$0.03557^{\{4\}}$	$0.03752^{\{6\}}$	$0.03339^{\{2\}}$
		$\hat{\lambda}$	$0.08672^{\{6\}}$	$0.09854^{\{7\}}$	$0.07861^{\{3\}}$	$0.07575^{\{1\}}$	$0.10038^{\{8\}}$	$0.08563^{\{4\}}$	$0.08624^{\{5\}}$	$0.07835^{\{2\}}$
	$\sum Ranks$		$33^{\{5.5\}}$	$42^{\{7\}}$	$13^{\{3\}}$	$12^{\{2\}}$	$48^{\{8\}}$	$24^{\{4\}}$	$33^{\{5.5\}}$	$11^{\{1\}}$

Table 9. Partial and overall ranks of the classical estimation methods for several parametric values.

$\vartheta^{\top}$	n	WLSE	OLSE	MLE	MPSE	CVME	ADE	RADE	PCE
	30	5	6	3	1	7	2	4	8
	80	5	6	1.5	1.5	7	3	4	8
$(\delta = 0.45, \lambda = 0.50)$	120	5	6	1.5	1.5	7	3	4	8
	200	5	6	1.5	1.5	7	3	4	8
	350	5	6	1.5	1.5	7	3	4	8
	30	5	7	3	1	8	2	4	6
	80	5	6	2	1	8	3	4	7
$(\delta = 0.45, \lambda = 1.00)$	120	5	6	1.5	1.5	7	3	4	8
	200	5	6	1.5	1.5	7	3	4	8
	350	5	6	1	2	7	3	4	8
	30	5	7	3	1	8	2	4	6
	80	4.5	6	2	1	8	3	4.5	7
$(\delta = 0.45, \lambda = 1.75)$	120	4.5	6	2	1	7.5	3	4.5	7.5
	200	5	6	1.5	1.5	7.5	3	4	7.5
	350	5	6	1.5	1.5	7.5	3	4	7.5

Table 9. *Cont.*

$\boldsymbol{\vartheta}^{\top}$	n	WLSE	OLSE	MLE	MPSE	CVME	ADE	RADE	PCE
$(\delta = 0.45, \lambda = 3.00)$	30	4.5	6	3	1	7	2	4.5	8
	80	4	6	2	1	7	3	5	8
	120	4	6	1.5	1.5	7	3	5	8
	200	4.5	6	1.5	1.5	7	3	4.5	8
	350	4.5	6	1.5	1.5	7	3	4.5	8
$(\delta = 0.75, \lambda = 0.50)$	30	5	6	3.5	1	8	2	3.5	7
	80	5	6	2	1	7	3	4	8
	120	5	6	1.5	1.5	7	3	4	8
	200	5	6	1.5	1.5	7	3	4	8
	350	5	6	1.5	1.5	7	3	4	8
$(\delta = 0.75, \lambda = 1.00)$	30	5.5	7	3	1	8	2	4	5.5
	80	5.5	7	2	1	8	3	4	5.5
	120	5	7	2	1	8	3	5	5
	200	5	7	2	1	8	3	4	6
	350	5	7	1.5	1.5	8	3	4	6
$(\delta = 0.75, \lambda = 1.75)$	30	5	7	3	1	8	2	4	6
	80	4.5	6	2	1	8	3	4.5	7
	120	4.5	6	1.5	1.5	8	3	4.5	7
	200	4.5	6	1.5	1.5	8	3	4.5	7
	350	4.5	6	1.5	1.5	7	3	4.5	8
$(\delta = 0.75, \lambda = 3.00)$	30	5	6	3	1	8	2	4	7
	80	4.5	6	1.5	1.5	7	3	4.5	8
	120	4	6	1.5	1.5	7	3	5	8
	200	4	6	1.5	1.5	7	3	5	8
	350	4	6	1.5	1.5	7	3	5	8
$(\delta = 1.50, \lambda = 0.50)$	30	6	7	4	1	8	2	5	3
	80	6	7	2	1	8	3	5	4
	120	5.5	7	2	1	8	3	4	5.5
	200	5.5	7	2	1	8	3	4	5.5
	350	5	7	1.5	1.5	8	3	4	6
$(\delta = 1.50, \lambda = 1.00)$	30	6	7	3	1	8	2	5	4
	80	5	7	2	1	8	3	5	5
	120	5	7	2	1	8	3	5	5
	200	5	7	1.5	1.5	8	3	4	6
	350	5	7	1.5	1.5	8	3	4	6
$(\delta = 1.50, \lambda = 1.75)$	30	5.5	7	3	1	8	2	5.5	4
	80	4.5	7	1.5	1.5	8	3	4.5	6
	120	4.5	7	1.5	1.5	8	3	4.5	6
	200	4.5	6	1.5	1.5	8	3	4.5	7
	350	5	6	1.5	1.5	8	3	4	7
$(\delta = 1.50, \lambda = 3.00)$	30	5.5	7	3	1	8	2	5.5	4
	80	4	6.5	2	1	8	3	5	6.5
	120	4	6.5	1.5	1.5	8	3	5	6.5
	200	4	6	1.5	1.5	8	3	5	7
	350	4	6	1.5	1.5	8	3	5	7
$(\delta = 4.00, \lambda = 0.50)$	30	5	7	5	2	8	3	5	1
	80	6	7	3	2	8	4	5	1
	120	6	7	3	2	8	4	5	1
	200	6	7	2	2	8	4	5	2
	350	6	7	2	1	8	4	5	3

Table 9. *Cont.*

$\vartheta^{\top}$	n	WLSE	OLSE	MLE	MPSE	CVME	ADE	RADE	PCE
	30	6	7	4	1	8	3	5	2
	80	6	7	3	1.5	8	4	5	1.5
$(\delta = 4.00, \lambda = 1.00)$	120	5.5	7	2	3	8	4	5.5	1
	200	6	7	1	2	8	4	5	3
	350	6	7	1	2	8	4	5	3
	30	6	7	4	2	8	3	5	1
	80	5.5	7	3	2	8	4	5.5	1
$(\delta = 4.00, \lambda = 1.75)$	120	5.5	7	2.5	2.5	8	4	5.5	1
	200	6	7	2	3	8	4	5	1
	350	5.5	7	2	3	8	4	5.5	1
	30	5.5	7	4	1.5	8	3	5.5	1.5
	80	5	7	3	2	8	4	6	1
$(\delta = 4.00, \lambda = 3.00)$	120	5.5	7	3	2	8	4	5.5	1
	200	5	7	2	2	8	4	6	2
	350	5.5	7	3	2	8	4	5.5	1
$\sum$ **Ranks**		404	523	171	117.5	616.5	244	369.5	434.5
Overall Rank		5	7	2	1	8	3	4	6
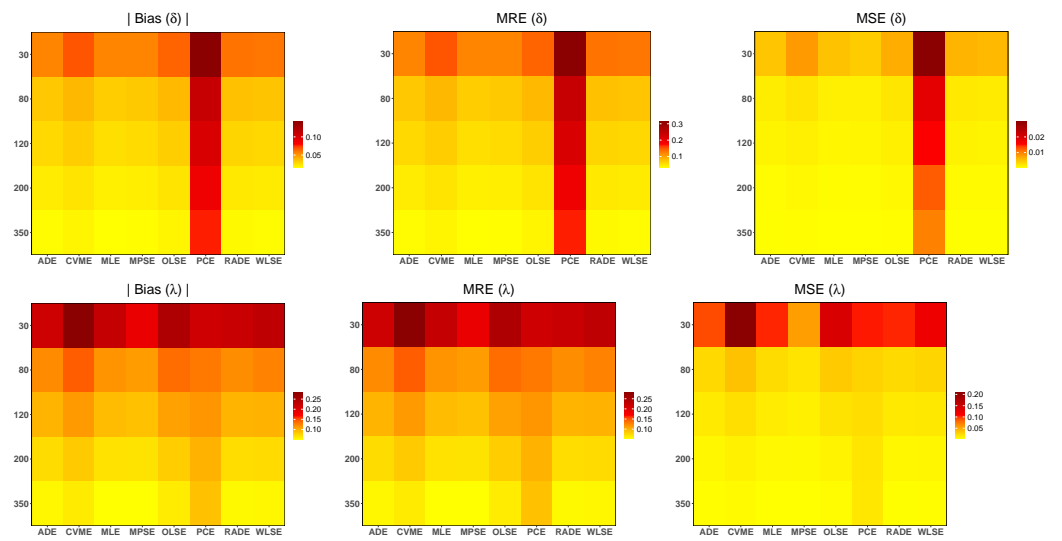
Figure 3. The heatmaps of the simulated biases, MSE and MRE of the eight simulation methods for $\delta = 0.45$ and $\lambda = 1.00$.
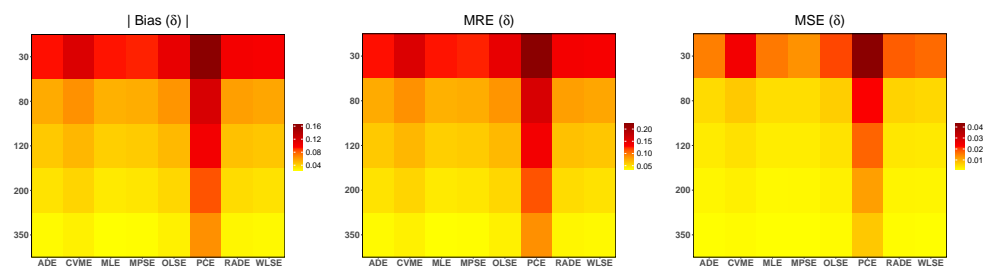
Figure 4. *Cont.*
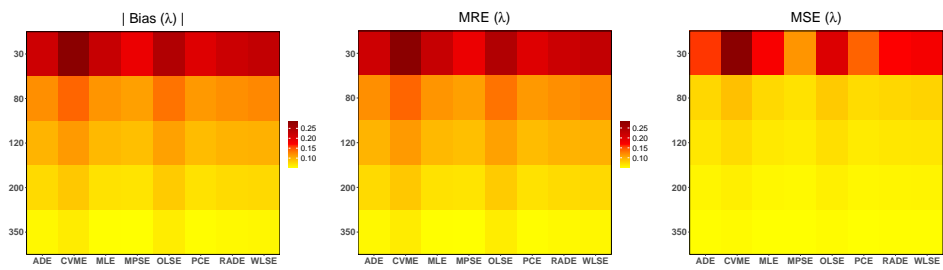
Figure 4. The heatmaps of the simulated biases, MSE and MRE of the eight simulation methods for $\delta = 0.75$ and $\lambda = 1.00$.
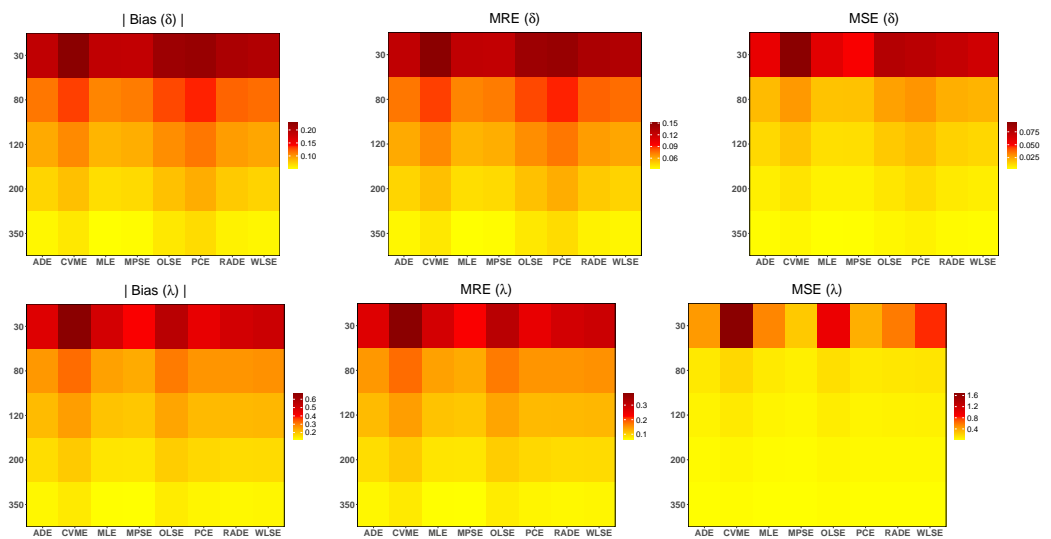
Figure 5. The heatmaps of the simulated biases, MSE and MRE, of the eight simulation methods for $\delta = 1.50$ and $\lambda = 1.75$.
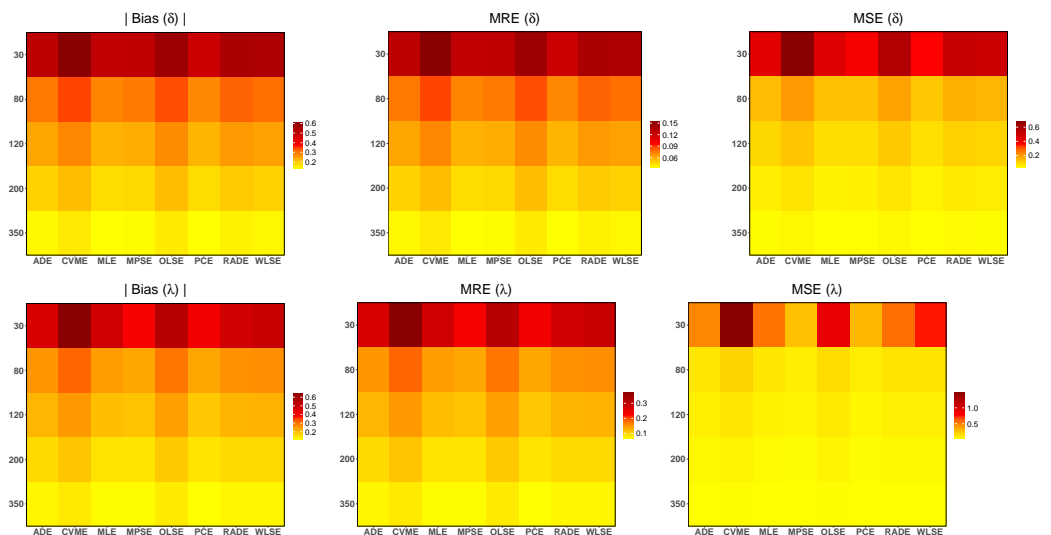
Figure 6. The heatmaps of the simulated biases, MSE and MRE, of the eight simulation methods for $\delta = 4.00$ and $\lambda = 1.75$.

5. Data Modeling

In this section, we carry out the practical evaluation of the WS-Weibull model. This fact is shown by choosing two data sets from the engineering sector. Both the data sets represent the failure times of the electronic components.

Using the failure time data sets, we compare the results of the WS-Weibull model with three other different well-known variants of the Weibull model. These models are given by the (i) exponentiated Weibull (for short "E-Weibull"), distribution, (ii) new exponential cosine Weibull (for short "NEC-Weibull") distribution, and (iii) logarithmic Weibull (for short "L-Weibull") distribution. The CDFs of the above-competing probability modes are expressed, respectively, by

$$G(x; \theta, \boldsymbol{\vartheta}) = \left(1 - e^{-\lambda x^{\delta}}\right)^{\theta}, \qquad x \geq 0, \theta > 0,$$

$$G(x; \beta, \boldsymbol{\vartheta}) = 1 - \cos\left(\frac{\pi}{2}\left[\frac{1 - e^{-\lambda x^{\delta}}}{1 - (1 - \beta)e^{-\lambda x^{\delta}}}\right]\right), \qquad x \geq 0, \beta > 0,$$

and

$$G(x; \alpha, \phi, \boldsymbol{\vartheta}) = 1 - \left(1 - \frac{\phi\left(1 - e^{-\lambda x^{\delta}}\right)}{\phi - \log\left[1 - e^{-\lambda x^{\delta}}\right]}\right)^{\alpha}, \qquad x \geq 0, \alpha, \phi > 0.$$

The comparison of the WS-Weibull, E-Weibull, NEC-Weibull, and L-Weibull distributions is made using four different selection criteria. The selection criteria are chosen with the aim of figuring out the most suitable model for the failure time data set. The selection criteria are given by

- Akaike information criterion:
  The Akaike information criterion (AIC) is a useful method for evaluating how close/well a model fits the given data. It provides estimates of the relative amount of information lost by a given probability model. Therefore, a model that loses less information is a mark of the best fitting. It is calculated as

  $$2k - 2\ell.$$

- Consistent Akaike information criterion:
  The consistent Akaike information criterion (CAIC) is another useful tool for comparing the quality of the model fitting. It is obtained as

  $$\frac{2nk}{n - k - 1} - 2\ell.$$

- Bayesian information criterion:
  The Bayesian information criterion (BIC) is another statistical criterion for choosing the best model among a set of competing models. Generally, a model with lower BIC is preferred. The value of the BIC is obtained as

  $$k \log(n) - 2\ell.$$

- Hannan Quinn information criterion:
  Another model-fitting criterion is the Hannan-Quinn information criterion (HQIC). It also measures the goodness of fit of a given probability model. The HQIC is obtained as

  $$2k \log[\log(n)] - 2\ell.$$

The numerical values of the above selection criteria are computed with the help of computer software called R-package using the BFGS method.

5.1. Data 1

The first data set has fifty observations and represents the failure times of 50 (in weeks) components. These data were originally reported by [28]. Later on, numerous authors analyzed this data set; see [29–31].

Corresponding to the first failure times data, some basic description measures are skewness = 2.306048, kurtosis = 9.408282, range = 48.092, minimum = 0.013, maximum = 48.105, mean = 7.821, median = 5.320, variance = 84.75597, standard deviation = 9.2063, 1*st* quartile = 1.390, and 3*rd* quartile = 10.043; the size of the data, say *n*, is 50. A visual description of the first failure times data set is presented in Figure 7.
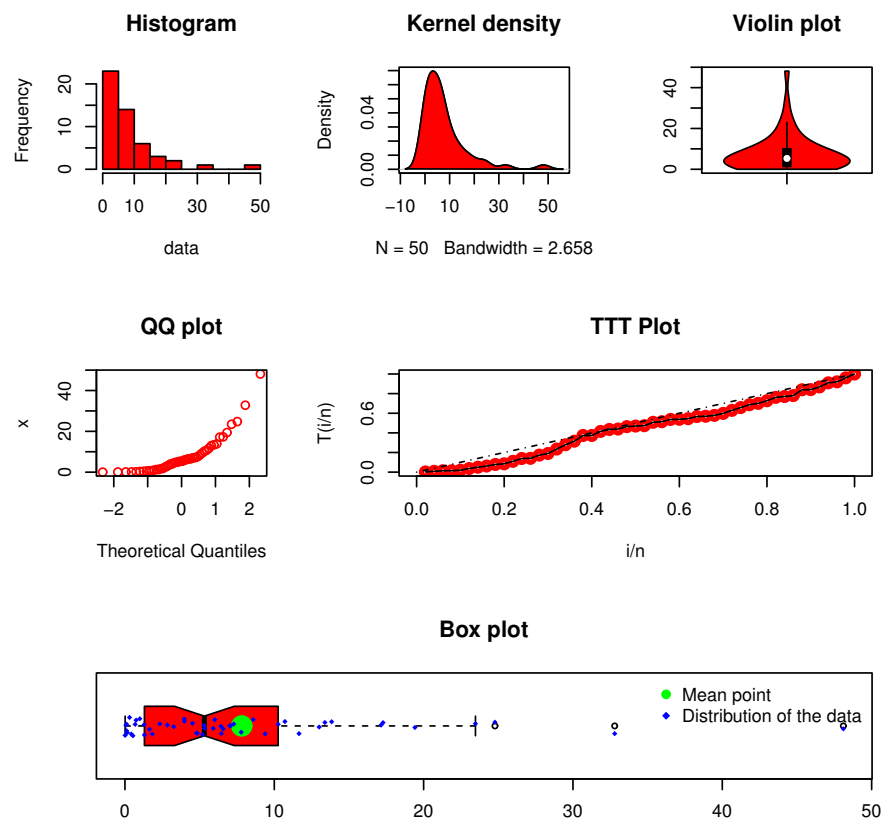
Figure 7. Visual description of the first failure times data set.

After analyzing the first data set, the values of $\hat{\delta}_{MLE}, \hat{\lambda}_{MLE}, \hat{\theta}_{MLE}, \hat{\alpha}_{MLE}$, and $\hat{\beta}_{MLE}$ are presented in Table 10. A visual display of the profiles of the LLF of $\hat{\delta}_{MLE}$ and $\hat{\lambda}_{MLE}$ of the WS-Weibull distribution is presented in Figure 8. The plots in Figure 8 reveal a unique solution of the MLEs of the WS-Weibull distribution.

Table 10. Using the first failure times data, the values of $\hat{\delta}_{MLE}, \hat{\lambda}_{MLE}, \hat{\theta}_{MLE}, \hat{\phi}_{MLE}, \hat{\alpha}_{MLE}$, and $\hat{\beta}_{MLE}$ of the fitted distributions.

| Models	$\hat{\delta}_{MLE}$	$\hat{\lambda}_{MLE}$	$\hat{\theta}_{MLE}$	$\hat{\phi}_{MLE}$	$\hat{\alpha}_{MLE}$	$\hat{\beta}_{MLE}$
WS-Weibull	0.84861	0.06628	-	-	-	-
E-Weibull	0.32947	1.39376	5.28710	-	-	-
L-Weibull	0.55268	0.55492	-	0.48751	1.22066	-
NEC-Weibull	0.42927	1.03216	-	-	-	2.96768
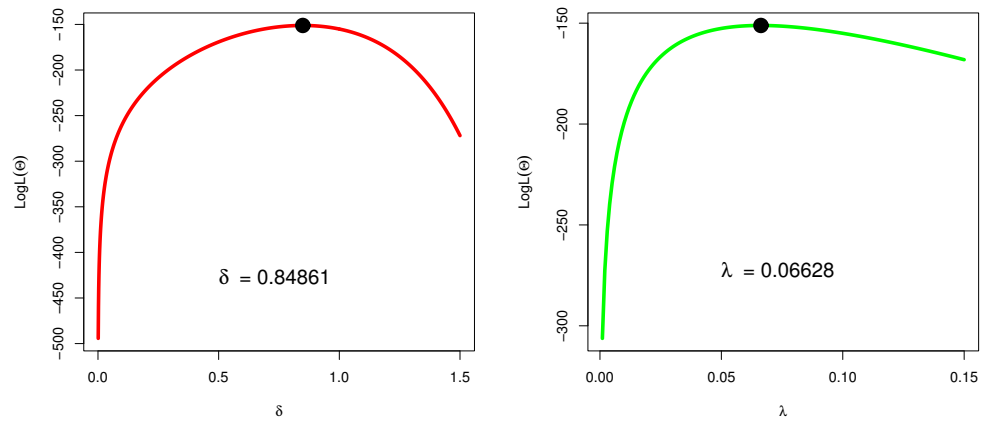
Figure 8. The profiles of the LLF of $\hat{\delta}_{MLE}$ and $\hat{\lambda}_{MLE}$ of WS-Weibull using the first failure times data.

Table 11 provides the values of the selection criteria of the WS-Weibull and other competing probability models. From the numerical description of fitted models in Table 11, it can be observed that the WS-Weibull is the best probability model for analyzing the failure data set. The second-best suitable model is the L-Weibull distribution. Whereas, the third-best model is the NEC-Weibull distribution.

After the numerical comparison of the WS-Weibull distribution and other variants of the Weibull distribution presented in Table 11, we also provide a visual illustration of the WS-Weibull distribution. For the visual comparison using the first failure times data, we select the plots of the fitted CDF, SF, PDF, quantile-quantile (QQ), and probability-probability (PP); see Figure 9. The visual description in Figure 9 reveals that the WS-Weibull distribution closely follows the first failure times data.

Table 11. For the first failure times data, the values of selection criteria of the competing distributions.

Models	AIC	CAIC	BIC	HQIC
WS-Weibull	306.28000	306.53530	310.10400	307.73620
E-Weibull	315.68840	316.21010	321.42440	317.87270
L-Weibull	309.23860	310.12750	316.88670	312.15110
NEC-Weibull	310.05400	310.57570	315.79000	312.23830
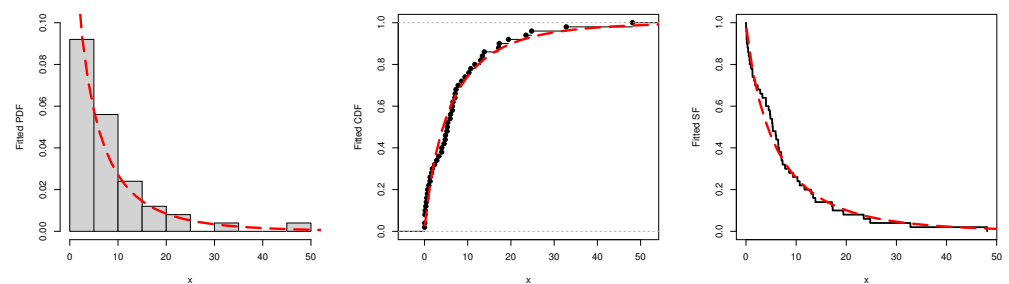
Figure 9. *Cont.*
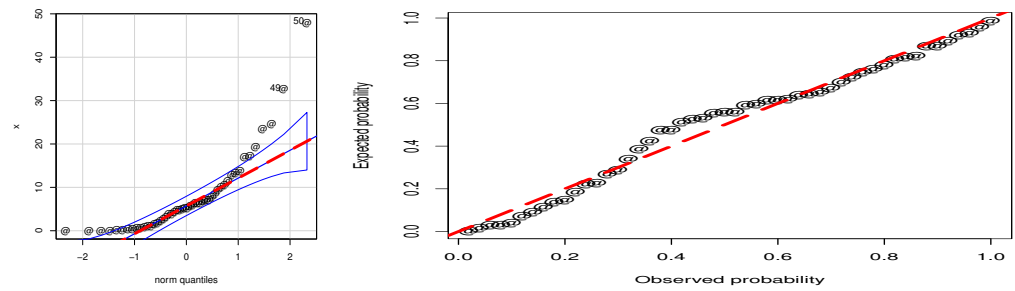
Figure 9. A visual illustration of the WS-Weibull distribution using the first failure times data.

5.2. Data 2

The second failure times data set also consists of fifty observations and represents the failure times of 50 (per 1000 h) components. These data were also originally reported by [28].

Linked to the second failure times data, the basic description measures are given by skewness = 1.416739, kurtosis = 4.084622, range = 15.044, minimum = 0.0360, maximum = 15.0800 mean = 3.3430, median = 1.4140, variance = 17.48477, standard deviation = 4.181479, 1*st* quartile = 0.2075, 3*rd* quartile = 4.4988, and *n* = 50. A visual description of the second failure time data set is provided in Figure 10.
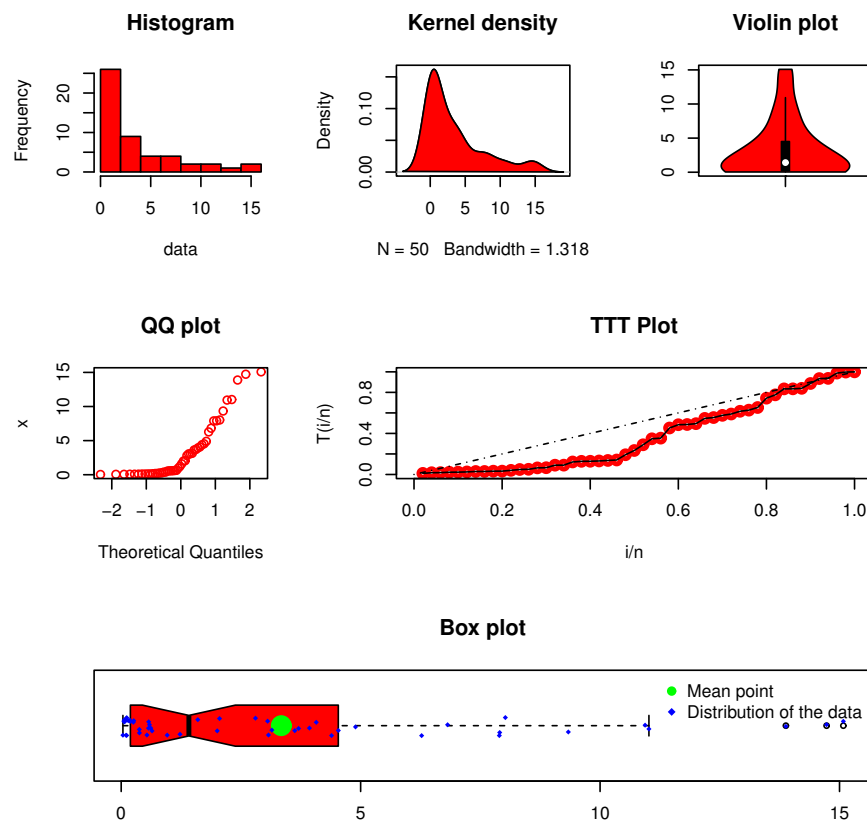
Figure 10. Visual description of the second failure times data set.

Corresponding to the second failure times data set, the numerical values of the MLEs $(\hat{\delta}_{MLE}, \hat{\lambda}_{MLE}, \hat{\theta}_{MLE}, \hat{\alpha}_{MLE}, \hat{\beta}_{MLE})$ are presented in Table 12. Furthermore, a visual display of the profiles of the LLF of $\hat{\delta}_{MLE}$ and $\hat{\lambda}_{MLE}$ of the WS-Weibull model is provided in Figure 11.

The plots of the profiles of the LLF in Figure 11 confirm a unique solution of $\hat{\delta}_{MLE}$ and $\hat{\lambda}_{MLE}$.
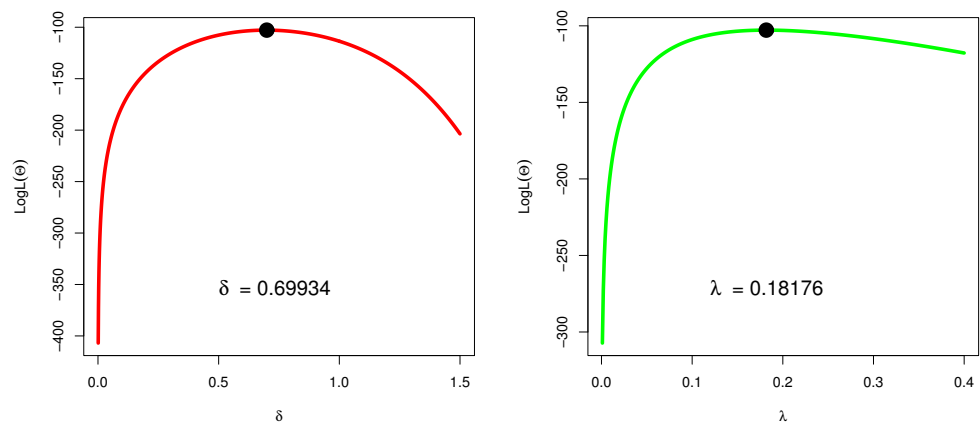
Figure 11. The profiles of the LLF of $\hat{\delta}_{MLE}$ and $\hat{\lambda}_{MLE}$ of WS-Weibull using the second failure times data.

Corresponding to the second failure times data, the values of the selection criteria of the WS-Weibull and other competing probability models are presented in Table 13. From Table 13, again, it can be observed that the WS-Weibull is the best probability model for analyzing the engineering data set.

In addition to the numerical comparison of the WS-Weibull distribution and other variants of the Weibull distribution, we show the performances of the WS-Weibull distribution visually. For the visual illustration of the WS-Weibull distribution, again we plotted the empirical CDF, SF, PDF, QQ , and PP; see Figure 12. Based on the visual description of the WS-Weibull distribution in Figure 12, we can observe that the WS-Weibull distribution closely fits the second failure times data.

Table 12. Using the second failure times data, the values of $\hat{\delta}_{MLE}, \hat{\lambda}_{MLE}, \hat{\theta}_{MLE}, \hat{\phi}_{MLE}, \hat{\alpha}_{MLE}$, and $\hat{\beta}_{MLE}$ of the fitted distributions.

Models	$\hat{\delta}_{MLE}$	$\hat{\lambda}_{MLE}$	$\hat{\theta}_{MLE}$	$\hat{\phi}_{MLE}$	$\hat{\alpha}_{MLE}$	$\hat{\beta}_{MLE}$
WS-Weibull	0.69934	0.18176	-	-	-	-
E-Weibull	0.53984	0.76136	1.37903	-	-	-
L-Weibull	0.10962	0.64226	-	5.09788	8.88077	-
NEC-Weibull	0.52723	0.57884	-	-	-	0.69887

Table 13. For the second failure time data, the values of selection criteria of the competing distributions.

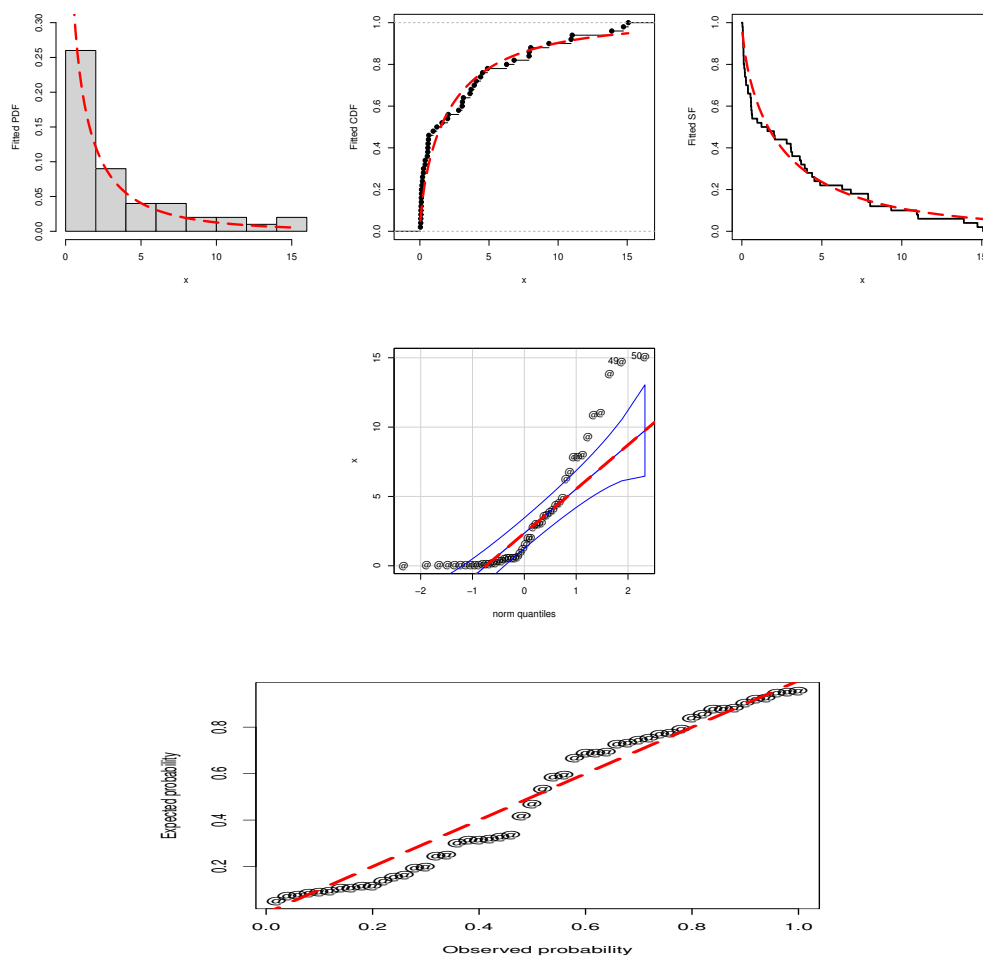| Models	AIC	CAIC	BIC	HQIC
WS-Weibull	208.60920	209.86460	213.43330	211.06550
E-Weibull	210.90750	211.42920	216.64350	213.09180
L-Weibull	212.46140	213.35030	220.10950	215.37390
NEC-Weibull	210.69880	211.22050	216.43490	212.88310

Figure 12. A visual illustration of the WS-Weibull distribution using the second failure times data.

6. Concluding Remarks

In recent times, the introduction of new families of distributions by using the trigonometric function has received great attention, especially thanks to the distributional flexibility in terms of modeling a wide variety of real data in applied sectors. In this study, we explore a new natural combination of sine-*G* and WT-*X* approaches. This combination led to a new method for generating new probability models named a weighted sine-*G* method. Thanks to the weighted sine-*G* method, it increases the distributional flexibility of the existing models without adding any new parameters. Certain distributional properties of the WS-*G* distributions are obtained. Based on the WS-*G* method, a new probability model, called the weighted sine-Weibull distribution, was studied. Eight different methods were implemented to estimate the parameters of the WS-Weibull distribution. After presenting distributional properties and simulation studies, we checked the practical ability of the WS-Weibull distribution by considering two engineering data sets. The practical applications demonstrate that the WS-Weibull distribution outperforms some well-established variants of the Weibull distribution.

Conflicts of Interest: The authors declare no conflict of interest.

References

1. Sindhu, T.N.; Atangana, A. Reliability analysis incorporating exponentiated inverse Weibull distribution and inverse power law. *Qual. Reliab. Eng. Int.* **2021**, *37*, 2399–2422. [CrossRef]
2. Liu, X.; Ahmad, Z.; Gemeay, A.M.; Abdulrahman, A.T.; Hafez, E.H.; Khalil, N. Modeling the survival times of the COVID-19 patients with a new statistical model: A case study from China. *PLoS ONE* **2021**, *16*, e0254999. [CrossRef]
3. Shen, Z.; Alrumayh, A.; Ahmad, Z.; Abu-Shanab, R.; Al-Mutairi, M.; Aldallal, R. A new generalized rayleigh distribution with analysis to big data of an online community. *Alex. Eng. J.* **2022**, *61*, 11523–11535 [CrossRef]
4. Moccia, B.; Mineo, C.; Ridolfi, E.; Russo, F.; Napolitano, F. Probability distributions of daily rainfall extremes in Lazio and Sicily, Italy, and design rainfall inferences. *J. Hydrol. Reg. Stud.* **2021**, *33*, 100771. [CrossRef]
5. Chen, P.; Ye, Z.S. Estimation of field reliability based on aggregate lifetime data. *Technometrics* **2017**, *59*, 115–125. [CrossRef]
6. Xu, A.; Zhou, S.; Tang, Y. A unified model for system reliability evaluation under dynamic operating conditions. *IEEE Trans. Reliab.* **2019**, *70*, 65–72. [CrossRef]
7. Zhang, L.; Xu, A.; An L.; Li, M. Bayesian inference of system reliability for multicomponent stress-strength model under Marshall-Olkin Weibull distribution. *Systems* **2022**, *10*, 196. [CrossRef]
8. Luo, C.; Shen, L.; Xu, A. Modelling and estimation of system reliability under dynamic operating environments and lifetime ordering constraints. *Reliab. Eng. Syst. Saf.* **2022**, *218*, 108136. [CrossRef]
9. Zhuang, L.; Xu, A.; Wang, X.L. A prognostic driven predictive maintenance framework based on Bayesian deep learning. *Reliab. Eng. Syst. Saf.* **2023**, *234*, 109181. [CrossRef]
10. Bantan, R.A.; Chesneau, C.; Jamal, F.; Elbatal, I.; Elgarhy, M. The truncated burr XG family of distributions: Properties and applications to actuarial and financial data. *Entropy* **2021**, *23*, 1088. [CrossRef]
11. Reyad, H.; Korkmaz, M.C.; Afify, A.Z.; Hamedani, G.G.; Othman, S. The Fréchet Topp Leone-G family of distributions: Properties, characterizations and applications. *Ann. Data Sci.* **2021**, *8*, 345–366. [CrossRef]
12. Eghwerido, J.T.; Agu, F.I. The shifted Gompertz-G family of distributions: Properties and applications. *Math. Slovaca* **2021**, *71*, 1291–1308. [CrossRef]
13. Eghwerido, J.T.; Nzei, L.C.; Omotoye, A.E.; Agu, F.I. The Teissier-G family of distributions: Properties and applications. *Math. Slovaca* **2022**, *72*, 1301–1318. [CrossRef]
14. Altun, E.; Alizadeh, M.; Yousof, H.M.; Hamedani, G.G. The Gudermannian generated family of distributions with characterizations, regression models and applications. *Stud. Sci. Math. Hung.* **2022**, *59*, 93–115. [CrossRef]
15. Kumar, D.; Singh, U.; Singh, S.K. A new distribution using sine function-its application to bladder cancer patients' data. *J. Stat. Appl. Probab.* **2015**, *4*, 417.
16. Mahmood, Z.; Chesneau, C.; Tahir, M.H. A new sine-G family of distributions: Properties and applications. *Bull. Comput. Appl. Math.* **2019**, *7*, 53–81.
17. Al-Babtain, A.A.; Elbatal, I.; Chesneau, C.; Elgarhy, M. Sine Topp-Leone-G family of distributions: Theory and applications. *Open Phys.* **2020**, *18*, 574–593. [CrossRef]
18. Jamal, F.; Chesneau, C.; Aidi, K. The sine extended odd Fréchet-G family of distribution with applications to complete and censored data. *Math. Slovaca* **2021**, *71*, 961–982. [CrossRef]
19. Jamal, F.; Chesneau, C.; Bouali, D.L.; Ul Hassan, M. Beyond the Sin-G family: The transformed Sin-G family. *PLoS ONE* **2021**, *16*, e0250790. [CrossRef]
20. Tomy, L.; Chesneau, C. The Sine Modified Lindley Distribution. Mathematical and Computational. *Applications* **2021**, *26*, 81.
21. Sakthivel, K.M.; Dhivakar, K. Transmuted Sine-Dagum Distribution and its Properties. *Reliab. Theory Appl.* **2021**, *16*, 150–166.
22. Muhammad, M.; Alshanbari, H.M.; Alanzi, A.R.; Liu, L.; Sami, W.; Chesneau, C.; Jamal, F. A new generator of probability models: The exponentiated sine-G family for lifetime studies. *Entropy* **2021**, *23*, 1394. [CrossRef] [PubMed]
23. Rajkumar, J.; Sakthivel, K.M. A New Method of Generating Marshall–Olkin Sine–G Family and Its Applications in Survival Analysis. *Lobachevskii J. Math.* **2022**, *43*, 463–472. [CrossRef]
24. Ahmad, Z.; Mahmoudi, E.; Dey, S.; Khosa, S.K. Modeling vehicle insurance loss data using a new member of TX family of distributions. *J. Stat. Theory Appl.* **2020**, *19*, 133–147. [CrossRef]
25. Alzaatreh, A.; Lee, C.; Famoye, F. A new method for generating families of continuous distributions. *Metron* **2013**, *71*, 63–79. [CrossRef]
26. Seneta, E. Karamata's characterization theorem, feller and regular variation in probability theory. P*Ublications L'Institut Math.* **2002**, *71*, 79–89. [CrossRef]
27. R Core Team. *R: A Language and Environment for Statistical Computing*; R Foundation for Statistical Computing: Vienna, Austria, 2022. Available online: https://www.R-project.org/(accessed on 31 October 2022).

28. Murthy, D.; Xie, M.; Jiang, R. *Weibull Models*; Wiley series in probability and statistics; John Wiley and Sons: Trenton, NJ, USA, 2004.
29. de Andrade, T.A.; Bourguignon, M.; Cordeiro, G.M. The exponentiated generalized extended exponential distribution. *J. Data Sci.* **2016**, *14*, 393–413. [CrossRef]
30. Gomes-Silva, F.; de Andrade, T.A.N.; Bourguignon, M. Ristić-Balakrishnan extended exponential distribution. Acta Scientiarum. *Technology* **2018**, *40*, e34963.
31. Tharshan, R.; Wijekoon, P. A modification of the Quasi Lindley distribution. *Open J. Stat.* **2021**, *11*, 369–392. [CrossRef]